Step-Growth Polyesters with Biobased (*R*)-1,3-Butanediol

Christopher A. DeRosa, ‡ Xiang Qi Kua, ‡ Frank S. Bates,† Marc A. Hillmyer ‡*

‡ Department of Chemistry, University of Minnesota, Minneapolis, Minnesota 55455-0431, United States

† Department of Chemical Engineering and Materials Science, University of Minnesota, Minneapolis, Minnesota 55455-0431, United States

KEYWORDS: Polycondensation, Step-Growth, Biobased, Polyester, Sustainability, Butylene Glycol, Polymer Microstructure

TOC Artwork

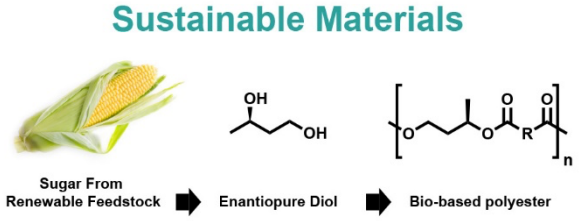

ABSTRACT

We present the synthesis and characterization of polymers containing 1,3-butanediol, also known as butylene glycol. Butylene glycol (BG) can be prepared from petroleum or sugar-based feedstocks. Petrol-based BG (petrol-BG) is isolated as a racemic mixture, whereas the biobased BG from sugar that we utilized (Bio-BG), is enantiopure upon purification (>99.7%). In the

presence of a titanium catalyst, polyesters were prepared by transesterification polymerization between petrol- or Bio-BG and various aliphatic and aromatic diacid derivatives. Polymers were analyzed by size-exclusion chromatography (SEC), ^{1}H NMR and ^{13}C NMR spectroscopies, thermogravimetric analysis (TGA), and differential scanning calorimetry (DSC). The synthesized polyesters were statistical in nature, according to ^{13}C NMR spectroscopy, a result of the asymmetric nature of the BG-starting material. As a result, many of the polyesters were amorphous in nature with low thermal glass transitions (T_g) and no melting points (T_m). In many of the polyester derivatives, the racemic petrol-based and enantiopure biobased BG polymers were nearly identical in thermal performance. Differences arose in semi-crystalline polyesters with long, aliphatic backbones (e.g., 1,14-tetradecanediocic acid; C14 diacid) or regioregular 4-hydroxybenzoate polyesters. This suggests the polymer microstructure (statistical versus sequenced) and the optical activity (racemic versus enantiopure) are important determinates in establishing the structure-property relationships in BG-containing polyesters. This work establishes synthetic protocols and the foundation for materials based on BG-containing polymers.

INTRODUCTION

Plastics have revolutionized the modern world.[1] This is because most plastics are inexpensive, durable, and versatile materials. However, the current consumption and accumulation of plastics are unsustainable.[2] The design of new materials must focus intensely on how polymers are made, used, and unmade to achieve a sustainable future.[3–7] Polyesters are an important class of polymers under investigation for sustainable material design due to the ability of ester bonds along the polymer backbone to readily decompose.[8,9] The most direct route to polyesters is through step-growth polymerization, performed routinely on an industrial scale.[10,11] Linear aliphatic diols, such

as 1,2-ethylene glycol (EG), 1,3-propanediol (PDO) and 1,4-butanediol (BDO), are important components in a wide variety of commercialized materials, such as poly(ethylene terephthalate) (PET) and poly(butylene succinate) (PBS).[12–16] These polymers are generally prepared from petroleum-based feedstocks, but over the years, biobased congeners or alternatives have been prepared.[1,6] For example, Miller and coworkers have reported a method for preparing terephthalic acid-based substitutes from bio-succinic acid in the generation of polymers with high glass transition temperatures (T_g) and high melting points (T_m).[17,18] Other examples include monomers from camphor,[19,20] α–limonene,[21,22] and (-)-menthol.[23,24] Other than the environmental advantages of being biobased, these monomers introduce optically active subunits into the polymer chain, which can significantly influence polymer microstructure and crystallinity.[25–29] Therefore, an investigation into new biobased substrates, especially monomers with high enantiopurity, can yield promising polymer properties (e.g., high degrees of crystallinity), or sustainable substitutes for existing polymer applications.[6,30–32]

Recently, a method for preparing biobased butylene glycol (i.e., 1,3-butanediol) has been developed on an industrial scale (**Figure 1**).[33,34] However, unlike the current mass-produced petrol-based butylene glycol, biobased butylene glycol can be acquired with 99.7% *R*-enantiopurity. This is likely a result of the synthetic starting materials; biobased butylene glycol (bio-BG) is prepared from glucose, whereas petrol-based butylene glycol (petrol-BG) is synthesized from acetaldehyde (**Figure 1**).[35] While acetaldehyde can be obtained from natural sources, the majority of it comes from petroleum sources, such as ethylene.[36–38] A life-cycle assessment study on the production of bio-BG and petrol-BG revealed a number of environmental drawbacks of the petrol-based derivative, such as increased global warming potential (103% greater) and higher energy demand than from non-renewable resources (85% greater).[39] A drawback to the biobased diol is an

increased acidification potential (50% greater), but this is a disadvantage shared with other plant-based polymers, such as poly(lactic acid) (PLA) and poly(hydroxy alkanoates) (PHA).[40] However, because of the different optical activities of BG-starting materials, the polymers prepared from different feedstocks may have distinct physical and thermal performance.

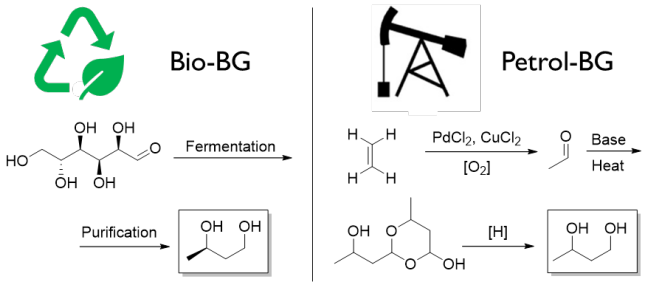

Figure 1. Industrial production of biobased (Bio-BG) and petrol-based (Petrol-BG) butylene glycol. Bio-BG is prepared via fermentation and isolation, whereas petrol-BG is prepared from oil-based ethylene.

Few polymers containing enantiomerically pure butylene glycol have been reported in the literature. Pérez and coworkers prepared aromatic BG-containing liquid crystalline polyesters, [41–43] which involved using biphenyl as a mesogen and enantiopure-BG as an alkyl-spacer to produce optically active materials. In another example, Yasuda and coworkers successfully prepared enantiomerically pure BG-containing polycarbonates *via* a cyclic-trimethylene carbonate monomer precursor.[44,45] The cyclic monomer could undergo ring-opening polymerization to yield relatively high molar mass homopolymers (M_n = 37.4 kDa, Đ = 1.5) or be copolymerized with ε–caprolactone and L-lactide to yield statistical copolymers (M_n = 40-130 kDa, Đ = 1.3-1.6). The BG-containing homopolymer carbonate showed a T_g of –1.7 °C, but no melting transition. However, structures like 1,3-butanediol have been investigated for copolymerizations, such as with 1,4-pentanediol and 1,2-propanediol.[46–48] In general, these studies on step-growth

polymerizations of methyl-branched diols are limited to the racemic mixture of isomers, and the role of optical activity was not established. To date, the structure-property relationships on BG-containing polymers, and step-growth polyesters in particular, have not been well-established.

Polyesters in this report are prepared by step-growth polycondensation between 1,3-butylene glycol (bio-BG or petrol-BG) and various aliphatic diacids (succinic, adipic, suberic, sebacic, and 1,14-tetradecanedioic acid) or aromatic diacids (2,5-furandicarboxylic acid and terephthalic acid) in the presence of a metal catalyst. Microstructure analysis by ^{13}C NMR spectroscopy showed the asymmetry of the bio-BG starting material yielded statistical polymers in select samples.[49,50] The statistical petrol- and bio-BG-based polyesters shared similarities in physical and thermal properties, which indicates the biobased congener is a suitable substitute for petrol-based polyesters in many situations. Statistical polymers with crystallinity, such as polymers with 1,14-tetradecanedioic acid, show higher melting points and evidence of polymorphism when the biobased enantiopure starting material is used. To prepare a regioregular polyester for comparison, the diol starting materials were converted to aromatic phenolic ethers with ethyl 4-hydroxybenzoate. Subsequent polymerization yielded highly crystalline materials (T_m > 200 °C). Herein, the synthesis and characterization of butylene glycol-based polyesters are investigated to determine the structure-property relationships between the enantiopure and racemic polymers.

RESULTS and DISCUSSION

Synthesis

Catalyst screening. Preparing polyesters via step-growth polymerization can require high temperatures over long periods of time and a precise stoichiometric balance between monomers.[51,52] Finding a catalyst to prepare high molar mass (>20 kDa) BG-containing polyesters is key. It is also necessary that the catalyst does not promote side reactions, such as elimination chemistry at the secondary alcohol position of BG.[53] To test transesterification catalysts, polymerizations were screened for the copolymerization between succinic acid and bio-BG (**Scheme 1**), yielding bio-poly(butylene glycol succinate) (bio-PBGS). A method was adapted by Jacquel and coworkers for the synthesis of poly(butylene succinate),[54] where the diacid and the diol are reacted first, then the metal catalyst is added to the reaction vessel before subjecting it to high vacuum. Succinic acid was chosen as a comonomer based on the higher glass transition temperature in previously reported polyesters.[17,55,56] Initial tests with diacid chlorides and diesters yielded low molar mass polymers compared to the diacid derivative. Mechanical stirring was adapted for these polymerizations as well to overcome the high melt viscosities of the polymerization (**Figure S1**). Purified polymers were analyzed by ^{1}H NMR spectroscopy and size exclusion chromatography (SEC using polystyrene standards).

Scheme 1. Copolymerization of bio-BG and succinic acid for catalyst screening

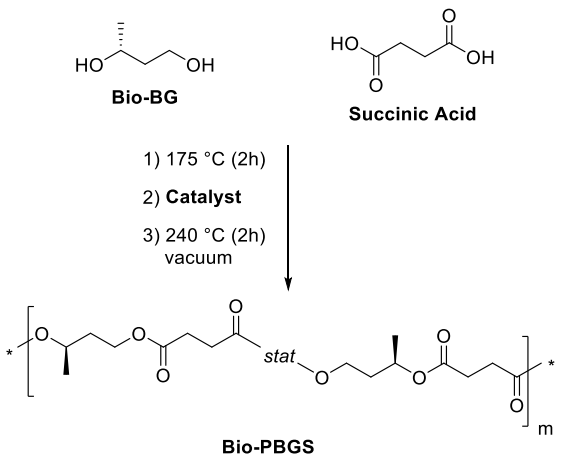

The copolymerization of bio-BG and succinic acid took place in two stages. In the first stage, bio-BG and succinic acid were mixed by mechanical stirring and the corresponding melt was heated to an elevated temperature (175 °C). During this step, esters are formed, and water vapor is removed as a by-product with a steady stream of nitrogen gas. According to SEC measurements, the molar mass plateaus at around 900 g/mol (75-85% conv.) after ~2 h. After maximum conversion without a catalyst, the transesterification catalyst was added. The catalysts (500 ppm to total mol content of bio-BG and succinic acid) were chosen based on literature precedent for this type of polycondensation.[53,55,57–60] After about 30 min to homogenize the mixture the reaction vessel temperature was heated to 240 °C over the course of 2 h while under dynamic vacuum to remove excess butylene glycol. The reaction time was kept to 2 h to reduce the number of possible side reactions involving the butylene glycol (e.g., elimination).[53] Catalysts such as triazabicyclodecene (TBD) and tosic acid (TsOH) were ineffective at producing high molecular mass polyesters according to SEC analysis (**Table 1** and **Figure S2**). Metal carboxylates (zinc and tin) produced low molar mass polymers (6–17 kDa). The highest performing catalysts were antimony and titanium-based molecules, achieving molar masses around 30-40 kDa. With

prolonged reaction times, the titanium catalyst led to yellowing of the polymer product, whereas the antimony catalyst resulted in colorless polymers albeit with lower molar masses (**Figure S3**). To produce the high molecular mass polymers with consistent properties, $Ti(OBu)_4$ was used for the remainder of the study. The reactions were closely monitored to minimize discoloration.

Table 1. Catalyst screening for bio-PBGS synthesis[a]

Catalyst	SEC-vs. PS[b]			Conv.[e] (%)	Yield[f] (%)	Appearance
	M_n[c] (g/mol)	M_w[c] (g/mol)	Đ[d]			
$Ti(OBu)_4$	38,000	87,200	2.3	>99	72	Colorless
Sb_2O_3[g]	29,300	54,300	1.9	>99	75	Colorless[g]
$Sn(Oct)_2$[h]	17,200	41,100	2.4	>99	63	Yellow
$Zn(OAc)_2$	6,800	13,800	2.0	98	61	Colorless
Li(acac)	4,700	7,100	1.5	89	12	Colorless
TBD	4,200	5,700	1.4	95	4	Colorless
TsOH	2,300	4,200	1.8	91	10	Tan
Neat[i]	1,700	3,700	2.2	95	96[j]	Colorless

a. Standard conditions (2 hours at 175 °C under steady flow of $N_{2(g)}$ followed by the addition of 500 ppm catalyst and slowly ramped to 240 °C for 2 hours under vacuum)
b. Size-exclusion chromatography versus polystyrene standards (1.0 mL/min in THF at 25 °C)
c. Number-average molecular mass (M_n) and weight-average molecular mass (M_w)
d. Dispersity index (Đ = M_w/ M_n)
e. Conversion defined by the integration of the ^{1}H NMR spectrum
f. Yield after purification via precipitation from $CHCl_3$ solution into -40 °C MeOH (× 2) followed by drying in a vacuum oven at 60–70 °C overnight (10–24 h)
g. The antimony catalyst was insoluble in the organic solvent, and a filtering step (fine sintered frit) was added before precipitation. The polymer is still opaque after filtering, suggesting the presence of $Sb_2O_{3(s)}$ particulates
h. $Sn(oct)_2$ is also known as tin(II)2-ethylhexanoate
i. Same reaction conditions without catalyst yielding bio-oligo-butylene glycol succinate. (bio-OBGS)
j. Not purified by precipitation and analyzed as prepared (crude)

Temperature-dependent polymerization. The reaction kinetics for the copolymerization of bio-BG and succinic acid were monitored to achieve two goals. First, by monitoring the reaction by ^{1}H NMR spectroscopy, the end-groups of the polymer can be resolved and used for additional experiments, such as polymerizing a second component,[61] or forming crosslinked thermosets.[62]

Second, observation of by-products or undesirable peaks in the ^{1}H NMR spectra will indicate a temperature or time threshold at the conditions being monitored. The kinetics for the polycondensation of bio-BG and succinic acid were measured at 200 °C and 240 °C with $Ti(OBu)_4$ (250 ppm). These temperatures are routinely used in step-growth polyesters and are well below the thermal decomposition of similar aliphatic polyesters found in the literature ($T_{5\%}$ = ~300 °C).[63] The catalyst loading was decreased in order to observe changes over a longer period of time (7h). Incremental aliquots (two per time point) were drawn for ^{1}H NMR spectroscopy and SEC analysis. By monitoring the BG-methine peak in the ^{1}H NMR spectrum (~5.0 ppm), the polymerization conversion was tracked as a function of time (see **Figure S4**).

Analysis of the aliquots by ^{1}H NMR spectroscopy revealed step-growth reaction kinetics, where high molar mass is achieved at conversions > 99% (**Figures S5** and **S6**).[51] At the elevated temperature of 240 °C, the polymerization occurs more rapidly at first, but also decomposes at longer reaction times (**Figure 2**). More noticeable is the color of the resultant polymers. The bio-PBGS polymer prepared at 200 °C remained mostly colorless, with only a slight browning effect (**Figure S7**), in contrast to the polymer prepared at 240 °C which was dark yellow in appearance. The ^{1}H NMR spectra of the final polymers suggest the formation of by-products is the source of the yellowing. Olefinic peaks are present in the final polymer when the reaction is performed at 240 °C, whereas the polymer prepared at 200 °C showed no unexpected peaks attributed to the formation of by-products. Therefore, longer reaction times at lower temperatures are ideal for this polymerization. For the remainder of polymerizations reported in this study, reaction temperatures were kept below 240 °C to mitigate undesirable side-reactions.

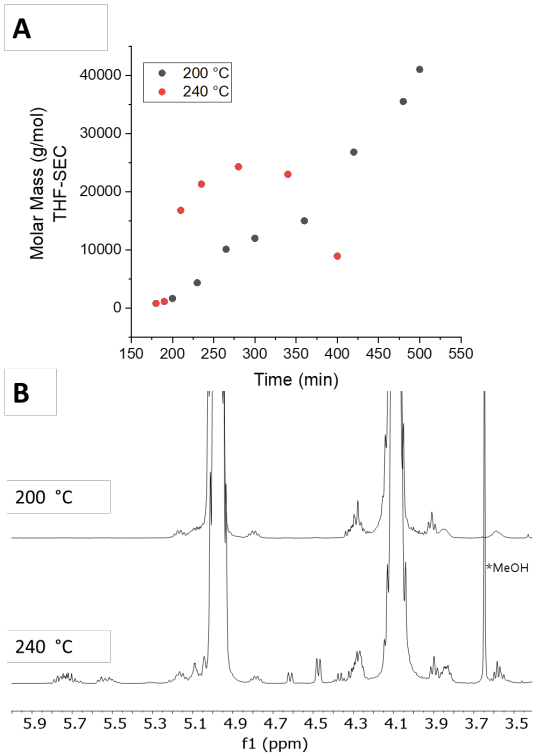

Figure 2. Temperature-dependent polymerization of bio-PBGS. A) Molar mass over time determine by THF SEC (1.0 mL/min) versus PS standards. B) ^{1}H NMR spectra of the final products from polymerization temperatures at 200 ℃ (top) and 240 ℃ (bottom).

Closer analysis of the aliquots by ^{1}H NMR spectroscopy revealed key proton signals, predicted in **Figure 3**. Before the polymerization takes place (0 min), the bio-BG methine peak is present as a single signal (labeled blue). Upon esterification at the secondary or primary alcohol positions, the chemical shift splits, labeled red and gold (**Figure 2**). These peaks emerge in the beginning stages of the polymerization, then diminish at higher conversions forming the disubstituted bio-BG, labeled green. In the final bio-PBGS polymer product, the red and gold peaks are maintained in the baseline, suggesting the alcohol end group is retained during the polymerization. Multi-dimensional heteronuclear NMR spectroscopy of the low molar mass oligomer (bio-OBGS) was used to confirm these proton assignments (**Figures S8-S11**). These assignments are also in good agreement with carbonate-based polycarbonates reported by Hua and coworkers[64] and Gregory and coworkers[65] Residual signals on the mono-substituted diols are

present in the final product, indicating this will facilitate any postpolymerization modification (e.g., chain extension).

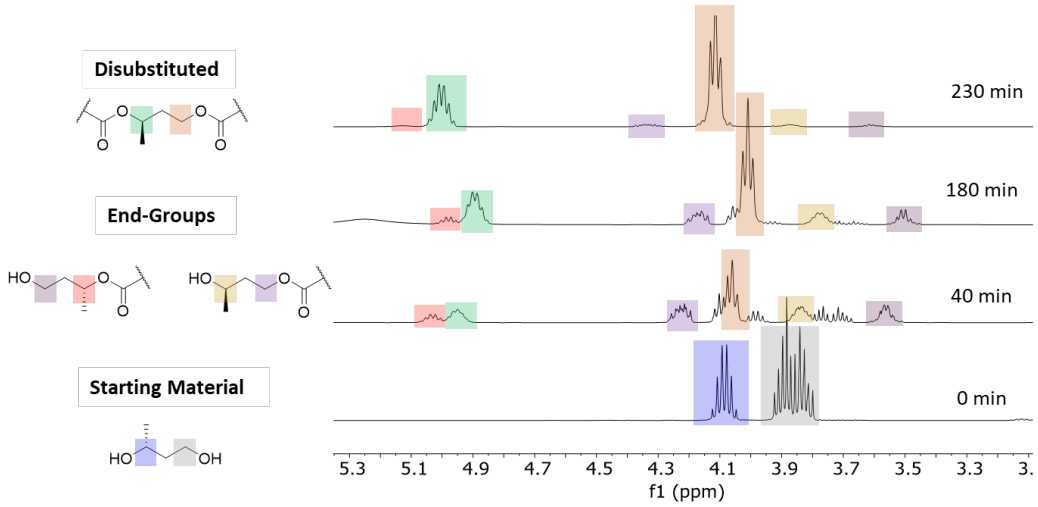

Figure 3. Key ^{1}H NMR spectroscopy ($CDCl_3$, 400 MHz) of signals from the end-groups from bio-BG during copolymerization with succinic acid. (Signal assignment facilitated by 2D NMR spectroscopy of the bio-OPBGS**; Figures S8-S11**).

Polyester synthesis. After determining a promising catalyst and temperature limits for the preparation of high molar mass bio-PBGS, the same reaction considerations were applied to other diacid derivatives of varying alkyl chain length (C4; succinic, C6; adipic, C8; suberic, C10; sebacic, and 1,14-tetradecanedioic acid; C14). Also, the racemic petrol-BG congeners were prepared (**Scheme 2**)**.** From here on, polyesters with enantiopure-BG are referred to as Bio-Polyesters (e.g., bio-PBGS), and polyesters with racemic-BG are referred to as petrol-polyesters (e.g., petrol-PBGS). Even-chained diacids were chosen based on literature precedence; even-chained diacid linkers show higher melting points compared to the odd-chained versions, therefore, changes induced by enantiopurity will likely have a greater impact on the thermal properties of these polyesters.[17,20,56,66] Terephthalates and furan-2,5-dicarboxylic acid monomers (FDCA) were chosen as comonomers for butylene glycol-based polymers as well. This range of

butylene glycol-based polymers was selected to help establish initial structure-property relationships. For comparison purposes, three polymers from different diols were prepared as well; poly(propylene succinate) (PPS), poly(butylene succinate) (PBS) and poly(2-methyl,1,3-propylene succinate) (PMPS). These model compounds facilitate establishing the role of the methyl group in the structure-property relationships as well.

Scheme 2. Synthesis of BG-containing polyesters. For explanation of acronyms, see **Table 2**.

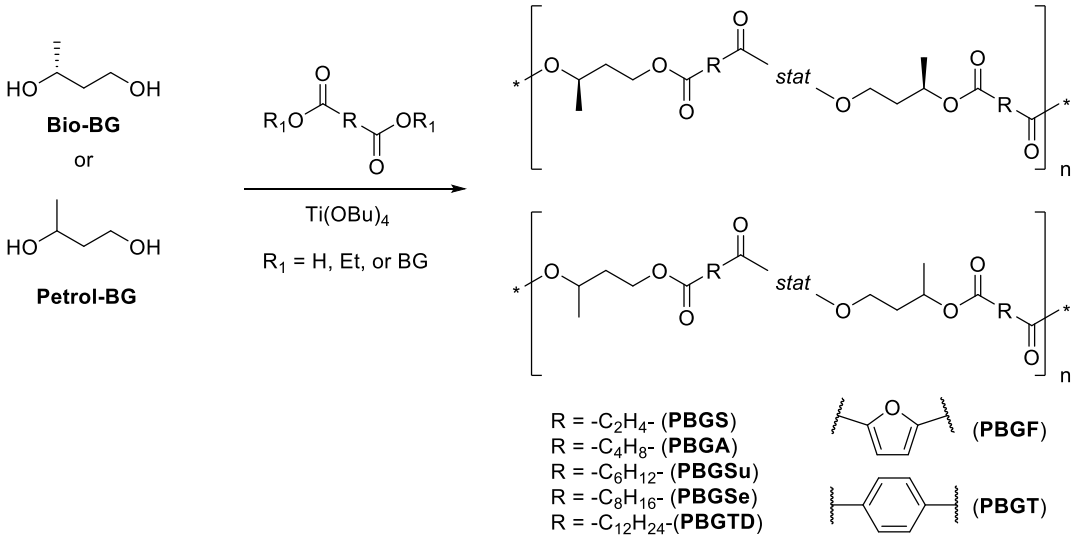

For the aliphatic polyesters (C4-C14), polymerizations with $Ti(OBu)_4$ yielded polymers with molar masses ranging from 14–60 kDa (**Table 2**) with no clear trends in molar mass observed. Fortuitously, the molar masses according to size-exclusion chromatography with multi-angle laser light scattering (SEC-MALLS) and the standard calibration curve (vs. PS standards) were in good agreement. The dispersity of the polymers was typical for step-growth polymerizations (Đ = 1.3-2.4). Lower molar mass polymers tended to not precipitate as readily compared to high molar mass samples, resulting in lower yields for those samples (e.g., Bio-PBGSu; M_n = 15.7 kDa, Yield =

23%). In general, the petrol- and biobased polyesters have comparable molar masses and similar dispersity values, indicating it is appropriate to compare the thermal properties of these materials. More importantly, the polymers are of high enough molar mass for comparison to industrially relevant polymers, such as poly(butylene succinate)[16] and poly(ethylene terephthalate).[67] The same reaction method was used to prepare the reference polymers as well (M_n according to SEC; PPS = 48kDa, PBS = 62 kDa, and PMPS = 47 kDa). Most of the aliphatic polymers were acquired as polymer melts, suggesting the glass transition temperature (T_g) is below room temperature. The C14-diacid derived polyesters (petrol and bio-PBGTD) were an exception, being isolated as white solids.

Table 2. Molar mass characterization of polyesters[a]

Polymer	Diacid Derivative[b]	M_n[c] (g/mol)	M_w[c] (g/mol)	Đ[d]	Yield[e] (%)	Appearance[f]
Bio-PBGS	C4	48,700	63,300	1.3	76	Colorless
Bio-PBGA	C6	34,700	52,100	1.5	70	Colorless
Bio-PBGSu	C8	15,700	20,400	1.3	23	Colorless
Bio-PBGSe	C10	29,000	37,700	1.3	70	Colorless
Bio-PBGTD	C14	49,700	74,700	1.5	92	White
Bio-PBGT	terephthalic	21,600	36,100	1.7	95	White
Bio-PBGF	FDCA	15,100	22,200	1.5	95	Yellow
Bio-PBGF	dE-FDCA[g]	9,800	19,200	2.0	63	White
Petrol-PBGS	C4	26,500	34,500	1.3	60	Colorless
Petrol-PBGA	C6	18,900	22,700	1.2	64	Colorless
Petrol-PBGSu	C8	14,000	18,200	1.3	40	Colorless
Petrol-PBGSe	C10	33,800	47,300	1.4	71	Colorless
Petrol-PBGTD	C14	33,500	50,300	1.5	90	White
Petrol-PBGT	terephthalic	21,000	30,000	1.4	95	White
Petrol-PBGF	FDCA	15,300	23,000	1.5	90	Yellow
PMPS	C4	47,400	71,300	1.5	77	Colorless
PPS	C4	48,300	87,000	1.8	97	Tan
PBS	C4	62,000[h]	149,000[h]	2.4[h]	92	White

a. Polyesters prepared using $Ti(OBu)_4$ as a catalyst
b. Diacid used in the polymerization
c. Size-exclusion chromatography equipped with multi-angle laser light scattering (SEC-MALLS), 1.0 mL/min THF at 25 °C. dn/dc was determined by assuming 100% mass recovery by single-point injection. Number-average molecular mass (M_n), weighted-average molecular mass (M_w),
d. Dispersity index ($Đ = M_w/ M_n$)
e. Yield after purification via precipitation from $CHCl_3$ solution into -40 °C MeOH (× 2) followed by drying in a vacuum oven at 60 - 70 °C overnight (10-24h)
f. All "colorless" polymers were isolated as polymer melts; "white", "yellow" and "tan" products were isolated as solids
g. Diethyl 2,5-furandicarboxylate was used in place of 2,5-furandicarboxylic acid
h. Determined by $CHCl_3$-SEC (1.0 mL/min at 35 °C) versus PS standards

The biobased furandicarboxylate polymer (Bio-PBGF) could be prepared as previously described for the aliphatic polyesters with several changes. First, five equivalences of bio-BG to 2,5-furandicarboxylic acid (FDCA) were used, and the titanium catalyst was present for the initial dehydration stage. The polymerization was run overnight at 175 °C (11 h) to dissolve the FDCA.

After heating overnight at 175 °C, the temperature was ramped slowly to 240 °C over the course of 4 h. Unlike the polymerization at 240 °C for bio-PBGS, no by-products were observed in the ^{1}H NMR spectra of the purified bio-PBGF polymer. The reaction was subjected to high vac (100 mTorr) for 0.5 h before cooling to room temperature, and purification to yield a yellow solid (~15 kDa). After several trials with FDCA (**Table S1** and **Figure S12**), to prepare colorless bio-PBGF we found substituting the diester version of FDCA (diethyl 2,5-furandicarboxylate; dE-FDCA) and keeping the reaction temperature below 200 °C yielded a white polymer solid after over 30h of reaction time (M_n (SEC) = 9.8 kDa; **Table 1** and **Figure 4**). This is the same approach reported by Avantium for preparing optically clear, furan-containing polyesters.[68] The polymer retained its white appearance after melt processing, suggesting that keeping a low temperature and minimizing the carboxylic acid groups could be key factors for achieving optically clear FDCA-containing polyesters.[54] Alternatively, a ring-opening polymerization approach could be adapted with bio-BG and FDCA to prepare optically clear, high molar mass polymers.[69]

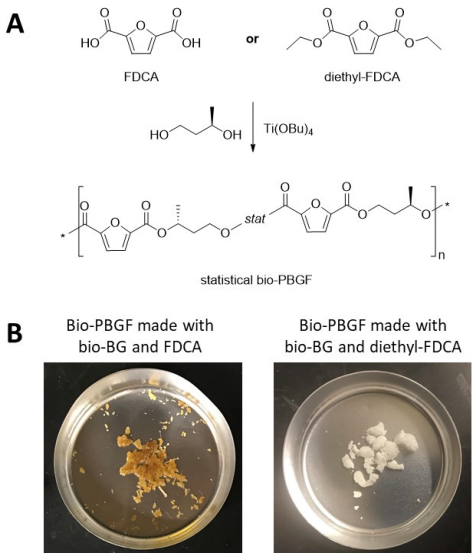

Figure 4. Images of bio-PBGF polyesters A) Scheme showing preparations of bio-PBGF polymers with $Ti(OBu)_4$. Note: the structure of the resultant polymers is the same (statistical bio-PBGF). B) Images of statistical bio-PBGF from FDCA and diethyl-FDCA starting materials. Samples were dried in a vacuum oven at 70 °C overnight prior to the images being taken with an iPhone 6**.**

The terephthalic acid showed limited solubility in bio-BG and petrol-BG. As a result, no conversion from starting materials to polymer was observed, even after overnight heating and with 20 equivalences of bio-BG. Therefore, to make the bio-terephthalate polyester, the diester had to be formed first with terephthaloyl chloride (**Scheme 3**). Interestingly, the bis-BG terephthalate intermediate (*bis*-bio-BGT) was > 99% selective for the primary alcohol during acetylation with terephthaloyl chloride, (**Figure S42**) and could be isolated in >70% yield after recrystallization. Subsequent polymerization yielded the BG-terephthalate polymer as a white solid (bio-PBGT; ~20 kDa). Direct polycondensation with terephthaloyl chloride and bio-BG resulted in low molar masses and brown products.

Scheme 3. Synthesis of BG-containing terephthalate-polyesters

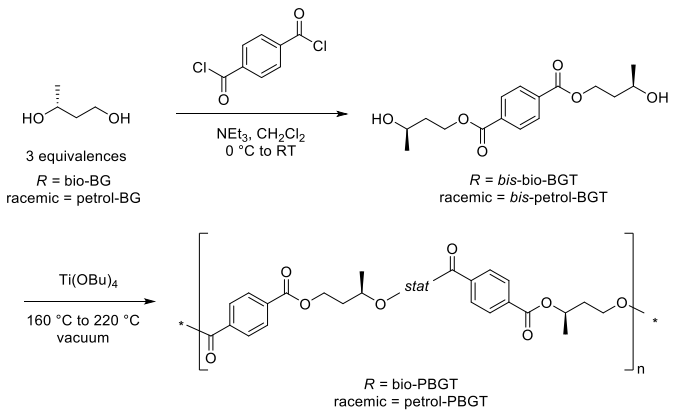

Polymer microstructure. The polymer sequence can have numerous effects on the thermal and mechanical properties of polymers.[70–73] Butylene glycol is an "A-B"-type monomer resulting in variable linkages across the polymer backbone. This leads to "head-to-tail" (HT), "head-to-head" (HH), or "tail-to-tail" (TT) microstructures. While the pre-polymer was shown to be regio-enriched, the bio-PBGT polymer was statistical according to ^{13}C NMR spectroscopy (**Figure 5**). This is the nature of transesterification polymerization reactions; chain scission among the ester bonds results in the linkages exchanging readily, so any pre-organization of the linkages is lost during extended reaction times.[53] As a result, the pre-polymer with regioregularity becomes statistical upon polymerization. The statistical linkages through the polymer can also be observed in other BG-based polyesters, shown in **Figure 6** with bio-PBGS and bio-PBGF.

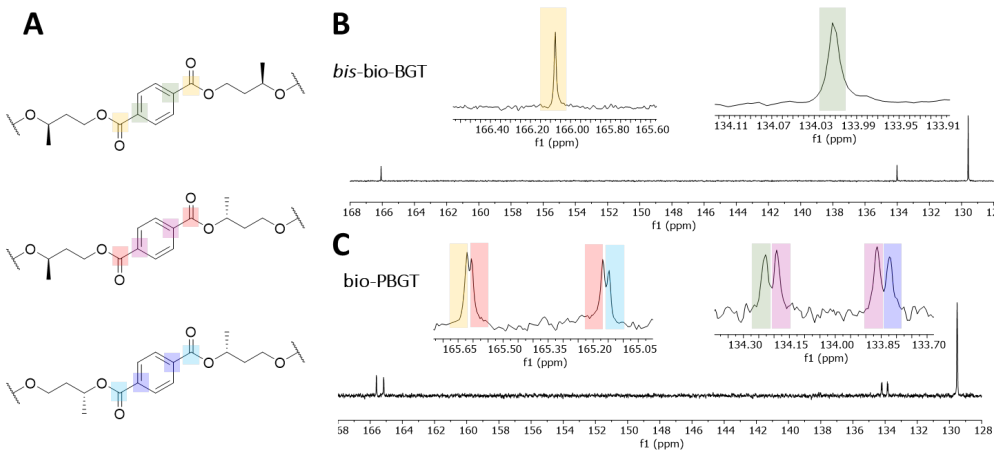

Figure 5. Statistical bio-PBGT microstructure. A) Schemes showing the different carbonyls and aromatic carbon signals for each structure along the polymer backbone resulting in transesterification. B) ^{13}C NMR spectra ($CDCl_3$, 101 MHz) of bis-bio-BG terephthalate monomer. The zoomed-in region shows a single carbonyl peak in the spectra. C) ^{13}C NMR spectra ($CDCl_3$, 101 MHz) of the bio-PBGT polymer. The expanded region shows multiple carbonyl peaks in the spectra responsible for the four carbonyl and aromatic carbon species (1 for HH, 2 for HT and 1 for TT). Assignments were facilitated by additional NMR spectroscopy experiments of similar polymers (**Figure S8-S11**)

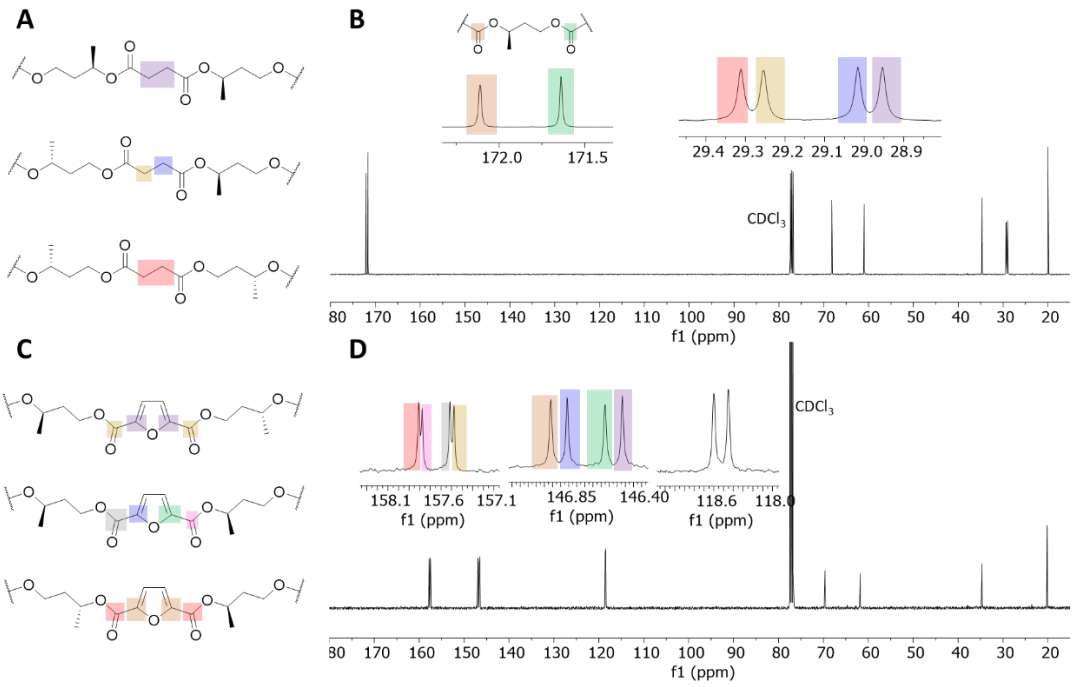

Figure 6. Statistical microstructure of bio-BG polyesters. A) Microstructure and associated carbon signals of bio-PBGS. B) ^{13}C NMR spectra ($CDCl_3$, 101 MHz) of the bio-PBGS polymer. Zoomed-in region shows multiple carbonyl peaks in the spectra responsible for the four carbonyl and aliphatic carbon species. C) Microstructure and associated carbon signals of bio-PBGF. D) ^{13}C NMR spectra ($CDCl_3$, 101 MHz) of the bio-PBGF polymer. The expanded region shows multiple carbonyl peaks in the spectra responsible for the four carbonyl and aromatic carbon species.

Thermal properties. The bio- and petrol-based polymers were characterized by thermogravimetric analysis (TGA) and differential scanning calorimetry (DSC). In general, the aliphatic petrol-based and the biobased statistical polymers have indistinguishable thermal properties (**Table 3**). The thermal decomposition at 5% mass loss (T_{dec}) of all the polymers is high under a nitrogen atmosphere, ranging from 290–350 °C. The T_g range from -60 to 60 °C of the polyesters depending on the diacid used (**Figure 7**). Aliphatic diacid chains generate a low T_g polymer (e.g. bio-PBGSe; T_g = -58 °C), whereas aromatic diacid units yield polymers with higher T_g's (e.g. bio-PBGF; T_g = 57 °C). The T_g of bio-PBGF is comparable to polylactide (T_g = 60 °C).[8,74] Compared to other FDCA copolymers with methyl-substituted diols, such as 2,2-dimethyl-1,3-

propanediol (T_g = 70 °C), the T_g for bio-PBGF is slightly lower (**Table S2**). The TGA and DSC analyses of the yellow, higher molar mass bio-PBGF from FDCA (M_n (THF-SEC) = 15.3 kDa) and the white, lower molar mass bio-PBGF from dE-FDCA (M_n (SEC) = 9.8 kDa) were similar, suggesting changes in molar mass or color were not significant enough to alter the thermal properties. No melting transition was observed in most of the polyesters.

Table 3. Thermal properties of polyesters[a]

Polymer	T_{dec}[b] (°C)	T_g[c] (°C)	T_m[c] (°C)	ΔH_m[c] (g/J)	T_c[d] (°C)	ΔH_c[d] (g/J)	T_{cc}[e] (°C)	ΔH_{cc}[e] (g/J)
Bio-PBGS	314	-22	-	-	-	-	-	-
Bio-PBGA	299	-48	-	-	-	-	-	-
Bio-PBGSu	336	-57	-	-	-	-	-	-
Bio-PBGSe	322	-58	-	-	-	-	-	-
Bio-PBGTD	345	-36	10, 37	36, 29	3	39	17	14
Bio-PBGT	320	40	-	-	-	-	-	-
Bio-PBGF[f]	308	57	-	-	-	-	-	-
Petro-PBGS	310	-23	-	-	-	-	-	-
Petro-PBGA	319	-48	-	-	-	-	-	-
Petro-PBGSu	340	-48	-	-	-	-	-	-
Petro-PBGSe	347	-58	-	-	-	-	-	-
Petrol-PBGTD	343	-32	10	45	4	46	-	-
Petro-PBGT	325	32	-	-	-	-	-	-
Petro-PBGF	309	63	-	-	-	-	-	-
P2MPS	268	-29	-	-	-	-	-	-
PPS	346	-27	48[g]	46	-	-	-	-
PBS	320	-[h]	114	64	87	69	104	5

a. DSC and TGA performed under $N_{2(g)}$ with a ramp heating rate of 10 °C/min
b. The onset temperature for decomposition under nitrogen at 10 °C/min (T_{dec}) determined by TGA and defined as 5% mass loss
c. Thermal glass transition (T_g) on the second cycle determined by DSC (10 °C/min, under N_2) Melting point (T_m) and enthalpy of fusion (ΔH_m) determined by DSC on the second heating cycle (10 °C/min, under N_2)
d. Crystallization point (T_c) and enthalpy of crystallization (ΔH_c) determined by DSC on the first cooling cycle (10 °C/min, under N_2)
e. Cold-crystallization temperature (T_{cc}) and enthalpy of cold-crystallization (ΔH_c) determined by DSC on the second heating cycle (10 °C/min, under N_2)
f. Thermal properties of bio-PBGF from FDCA comonomer
g. Melting transition observed only on the first cycle
h. Not observed

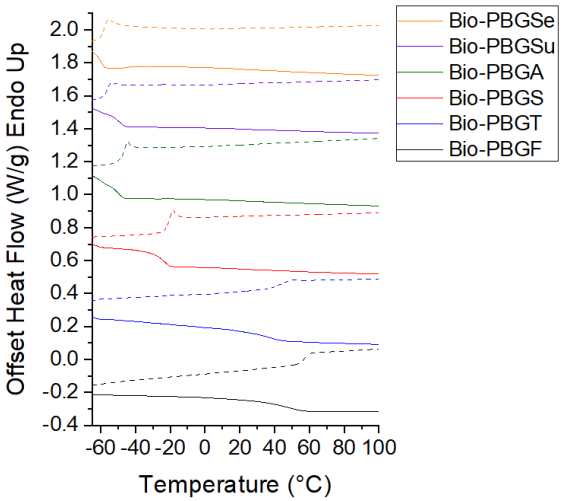

Figure 7. Differential scanning calorimetry of bio-BG polyesters (solid lines = 1st cooling cycle at 10 °C/min under N_2, dashed lines = 2nd heating cycle at 10 °C/min under N_2).Petro-based polyesters have similar DSC traces. Curves have been shifted vertically for clarity.

Unlike the other aliphatic polyesters, polymers prepared with 1,14-tetradecancedioic acid did yield semi-crystalline samples in both the petrol- and the biobased diol derivatives. With a C14-diacid, the tendency of the long aliphatic chains to crystallize dominates the defects introduced by the methyl groups or polymer microstructure (**Figure 8**).[75] After melting and cooling, both petrol-PBGTD and bio-PBGTD readily crystallized at about 3 ℃. Upon reheating (2nd cycle) the polymers melt at 10 ℃, at about the same temperature as the polymer from 1,4-pentanediol/1,14-tetradecanedioic acid as previously reported.[48] Upon heating, bio-PBGTD melts (T_m = 10 ℃), then rapidly cold crystallizes (T_{cc} = 17 ℃) and melts again at (T_m = 37 ℃). The T_{cc} and the second T_m are only present in the enantiopure, bio-BG polyester (bio-PBGTD). This suggests polymorphism that is only associated with the optically pure derivative. Given the narrow temperature range of the thermal transitions (3-37 ℃), there could be some potential for this polymer to be used in thermo-responsive materials, such as shape-memory biomaterials.[48,76–78] The temperature range is ideal for biological applications, where a polymer solid-to-liquid phase change would be induced around body temperature (37 ℃).[79–81] The polymers also provide

important insights into the structure-property relationships of step-growth polyesters; enantiopure starting materials can yield more crystalline polymers, even in regio-irregular polymers.

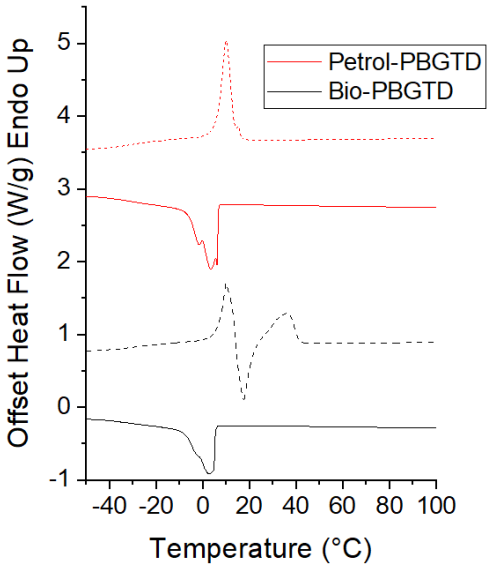

Figure 8. Differential scanning calorimetry of bio-PBGTD and petrol-PBGTD. Solid lines = 1st cooling cycle at 10 °C/min under N_2, dashed lines = 2nd heating cycle at 10 °C/min under N_2. Curves have been shifted vertically for clarity.

Comparing the BG-containing polymers to positional isomers, like 2-methyl 1,3-propanediol (MPDO), or the linear diols 1,4-butanediol (BDO) and 1,3-propanediol (PDO), can establish differences on structural properties of the diols. Reference polymers prepared with other diols and succinic acid were prepared (1,4-butanediol; PBS, 1,3-propanediol; PPS, and 2-methyl-1,3-propanediol; PMPS), as shown in **Figure 9** and **Table S3**. Linear polymers without the methyl group, PPS and PBS, show clear semi-crystalline properties with melting points at 48 °C and 114 °C, respectively. Surprisingly, PPS, the linear analog of PBGS, only exhibits a melting point on the first heating cycle and does not recrystallize quickly upon cooling at 5 °C min^{-1} or 10 °C min^{-1} cooling cycles. This suggests that polymers with a C3-carbon backbone are less likely to exhibit

polymer crystallinity.[56] Furthermore, polyesters with a methyl-group (bio-PBGS, petrol-PBGS, and PMPS), do not have any melting points. Also, the T_g values of PPS, PMPS, petrol-PBGS, and bio-PBGS all have similar values (≅ –25 °C). It is likely that both the odd-number carbon-chain backbone, the methyl-group, and the polymer microstructure (statistical versus regioregular) all contribute to the amorphous nature of the BG-based polyesters and achieving crystalline samples would need to account for these factors.

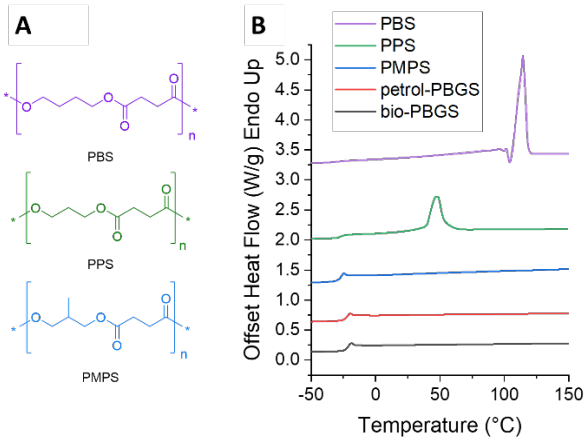

Figure 9. Differential scanning calorimetry comparison of varying polyesters. A). Chemical structures of reference polymers B) 2nd heating cycle (10 °C/min, under N_2). Curves have been shifted vertically for clarity.

Regio-Enriched Aromatic Polyesters. To prepare highly crystalline samples containing bio-BG, we focused on the polymer microstructure (statistical versus regioregular). Therefore, phenol-based ethers were targeted.[82] Phenolic ethers are easy to prepare and very stable under transesterification conditions. This was done by regioselective tosylation of the primary alcohol on BG, followed by Williamson ether synthesis with ethyl 4-hydroxybenzoate (**Scheme 4**).[82] This strategy could be extended to other aromatic phenols renewably sourced from lignin, such as vanillates and ferulates.[32,83,84] The synthesis of the petrol-derived monomer (*rac*-BGBz) was more

challenging to execute, involving separation columns after the tosylation and the ether synthesis. The bio-BG derivative readily crystallized from solution, and impurities, such as regioisomers, did not need to be removed by column chromatography. As a result, the total yield of the *R*-BGBz monomer was much higher (yield; *R*-BGBz = 42% vs *rac*-BGBz = 12%).

Scheme 4. Synthesis of regioregular poly(butylene glycol-4-hydroxybenzoate) (PBGBz)

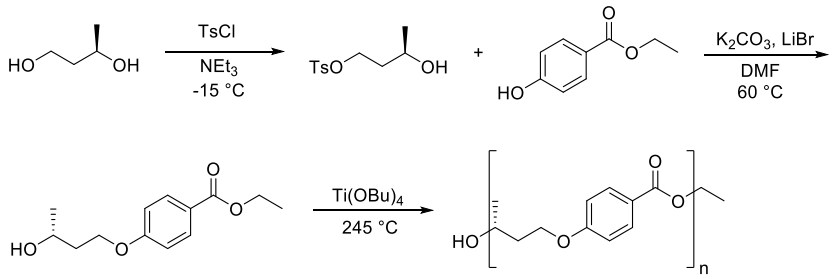

The polyester congeners (PBGBz; inset) were prepared by polycondensation with titanium tetrabutoxide at a maximum temperature of 245 °C after 24h. The reaction was performed without stirring due to the high crystallinity of the sample. At the end of the reaction, a yellow/brown product was purified by dissolution in $CHCl_3$/TFA and precipitated into cold methanol to yield a white powder. The resulting, regioregular polymers were around M_n = 1.5-3.0 kg/mol according to SEC in 1,1,1,3,3,3-hexafluoro-2-propanol (HFIP) and by ^{1}H NMR spectroscopy end-group analysis (**Table 4**). Varying the reaction temperature or time did not increase the polymer molar mass.

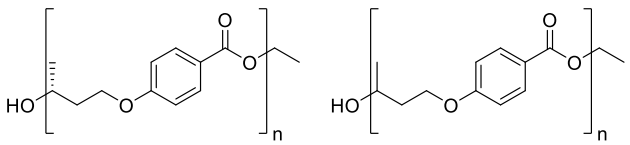

R-PBGBz *rac*-PBGBz

Table 4. Molar masses of *R*-PBGBz and *rac*-PBGBz

Polymer	M_n [a] (^{1}H NMR) (g/mol)	M_n [b] (SEC) (g/mol)	M_w [b] (SEC) (g/mol)	Đ[c]
R-PBGBz	4,400	2,400	8,900	3.7
rac-PBGBz	3,400	1,600	5,900	3.6

a. Number-average molar mass determined by ^{1}H NMR end group analysis
b. Number-average molar mass (M_n) and weighted-average molar mass (M_w) determined by HFIP-SEC (0.35 mL × min^{-1} at 40 °C) versus PMMA standards
c. Polymer dispersity (M_w/M_n)

The thermal properties of *R*-PBGBz and *rac*-PBGBz are summarized in **Table 5** and **Figure 10**. Both polymers have semi-crystalline properties. The *R*-PBGBz has a high melting temperature (T_m = 220 °C) and rapidly crystallized upon cooling (T_m = 185 °C). In contrast, *rac*-PBGBz has a melting point (T_m = 184 °C) and crystallizes upon re-heating (T_{cc} = 101 °C). It was surprising that the racemic-derived polymer (*rac*-PBGBz) has a melting point, as the racemic propylene glycol benzoate polymer (one less methylene group compared to butylene glycol) does not exhibit a melting point based on literature precedence (**Table S4**).[82] However, the data suggests the bio-derived polymer is more crystalline in nature with a higher T_m and T_c.

Table 5. Thermal properties of *R*-PBGBz and *rac*-PBGBz

Polymer	T_{dec}[a] (°C)	T_g[b] (°C)	T_m[c] (°C)	ΔH_m[d] (g/J)	T_c[e] (°C)	ΔH_c[f] (g/J)	T_{cc}[g] (°C)	ΔH_{cc}[h] (g/J)
R-PBGBz	320	-[i]	220	59	185	57	-	-
rac-PBGBz	299	37	184	54	101	16	101	31

a. The temperature at 5% mass loss determined by thermogravimetric analysis under $N_{2(g)}$
b. Glass transition temperature determined by DSC (10 °C/min, under N_2)
c. Melting point temperature determined by DSC (10 °C/min, under N_2)
d. Enthalpy of fusion determined by DSC (10 °C/min, under N_2)
e. Crystallization temperature determined by DSC (10 °C/min, under N_2)
f. Enthalpy of crystallization determined by DSC (10 °C/min, under N_2)
g. Cold crystallization temperature determined by DSC (10 °C/min, under N_2)
h. Enthalpy of cold crystallization determined by DSC (10 °C/min, under N_2)
i. The transition is not observed

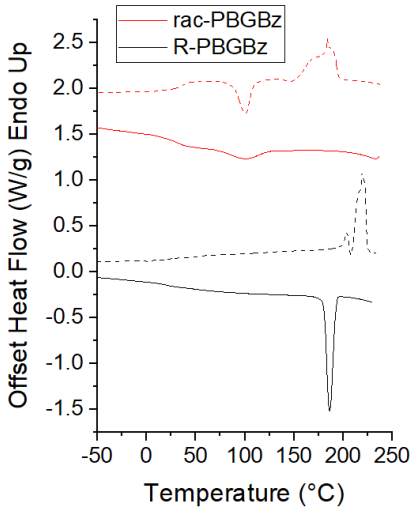

Figure 10. Differential scanning calorimetry (10 °C/min, under N_2) of rac- and *R*-PBGBz (solid lines = 1st cooling cycle at 10 °C/min, dashed lines = 2nd heating cycle at 10 °C/min).

CONCLUSION

The synthesis and characterization of a host of butylene glycol-based polyesters were conducted. Titanium tetrabutoxide ($Ti(OBu)_4$) was found to be the most effective catalyst for the transesterification polymerization between BG and various diacids (aliphatic and aromatic) to yield moderate to high molar mass polymers (M_n = 15-50 kDa). The resultant polymers of the

transesterification polymerization were entirely statistical in nature along the polymer backbone. The aliphatic polyesters were amorphous in nature (T_g = -60 to -20 °C), and glassy solids for the aromatic derivatives (T_g = 30 to 60 °C). The racemic petrol-BG and the enantiopure bio-BG were indistinguishable in terms of synthetic and thermal performance for the amorphous polymers. In semicrystalline samples prepared with 1,14-tetradecanedioic acid and 4-hydroxy-benzoates (PBGTD and PBGBz), polymers prepared with enantiopure-BG have higher melting points and greater enthalpies of melting.

MATERIALS and METHODS

Materials

Solvents CH_2Cl_2 and THF were dried via the Pure Process Technology Glass Contour Solvent Purification System (Solvent Column). Dimethylamide ($DMF_{(anhy.)}$) was used as received from Sigma-Aldrich. Enantiomerically pure (*R*)-(-)-1,3-butanediol was used as received from Genomatica. Racemic 1,3-butanediol was used as received from Daicel Corp. Related diols (1,4-butanediol, 1,3-propanediol, and 2-methyl, 1,3-propanediol) were purchased from Sigma-Aldrich and dried as previously described via vacuum-distillation over $MgSO_{4(s)}$.[85] Triethylamine (FisherBrand) was distilled over $K_2CO_{3(s)}$ prior to use.[85] Deuterated chloroform ($CDCl_3$) and deuterated TFA (*d*-TFA) were used as received from Cambridge Isotopes (99.7% deuterated). Initial polymerization attempts with the commercial grade diacids (>98% pure from Sigma) did not work initially. Therefore, aliphatic diacids were purchased from Sigma-Aldrich, recrystallized (~10:1 acetone/water) and dried in a vacuum oven for two days prior to use. The 2,5-furandicarboxylic acid (FDCA) was purchased from Ambeed and used as received. Diethyl 2,5-furandicarboxylate was prepared as previously described.[46] The catalyst, 1,5,7-

triazabicyclo[4.4.0]dec-5-ene (TBD), was sublimed twice prior to testing. The metal catalysts zinc acetate ($Zn(OAc)_2$), titanium tetrabutoxide ($Ti(OBu)_4$), antimony oxide$_{(s)}$ (Sb_2O_3), lithium acetylacetonate (Li(acac)), were purchased from Sigma-Aldrich and used without further purification. Stannous octoate ($Sn(oct)_2$) was purchased from Spectrum Chemical. Toluene sulfonic acid (TsOH) was dried via azeotropic distillation (dean-stark trap) in toluene for 24h at 140 °C. All other reagents were used as received from Sigma-Aldrich.

Methods

Polycondensation reactions were performed using a Heidolph mechanical stirrer (Hei-TORQUE Precision 100) equipped with a 10 mm diameter polished glass stir shaft, a vacuum adapter, and a PTFE swivel stirrer to fit in a 24/40 joint round-bottom flask. An aluminum block for a 100 mL-round bottom flask was used as the heating element. The reactions were insulated with insulating wool and aluminum foil throughout the polymerization. Representative polymerizations are described and annotated for all Bio-BG-based polymers. Nuclear magnetic resonance (NMR) spectra were recorded on a Bruker Advance III HD 400MHz Spectrometer equipped with an autosampler. Chemical shifts are reported in δ units, expressed in ppm using the residual protiochloroform signal (7.26 ppm) as an internal standard. For higher resolution in ^{13}C NMR (101 MHz) spectra to determine polymer microstructure, polymers were concentrated in $CDCl_3$ (~50 mg/mL) and the spectra were recorded with inverse-gated decoupling, a 1.5 second acquisition time and a 2.5-second relaxation delay for a total of 1024 scans. Before size-exclusion chromatography analysis, the polymer was dissolved in the HPLC-grade solvent (THF, $CHCl_3$, or HFIP/TFA) and filtered through a 0.2 nm filter (Whatman) before injection into the column. Size exclusion chromatography (SEC) in THF (1.0 mL/ min at 25 °C) was performed using an Agilent 1260 Infinity series HPLC equipped with a variable-wavelength UV-detector and three sytragel

columns (TOSOH). Molecular weights via THF-SEC were determined by conventional calibration vs. polystyrene standards or multi-angle laser light scattering (MALLS: Wyatt HELEOS II) and differential refractive index detectors (Wyatt; Optilab TrEX). The *dn/dc* values of the polymers in THF (25 °C, 658 nm) were determined using single point-injection, assuming 100% mass recovery of the injected polymer. Size exclusion chromatography in $CHCl_3$ (1.0 mL/ min at 35 °C) was performed using an Agilent 1100 series HPLC equipped with a UV diode-array detector with two styragel columns (Malvern) and the polymer molar masses were determined by conventional calibration versus polystyrene standards. Size exclusion chromatography in hexafluoroisopropanol (HFIP) containing 0.05 M potassium trifluoroacetate (0.35 mL/ min at 40 °C) was performed using a TOSOH EcoSEC Elite HLC-8420 GPC system with two Tosoh TSKgel SuperAWM-H, 9 μm, mixed-bed columns and the polymer molar masses were determined by conventional calibration versus poly(methyl methacrylate standards). Differential scanning calorimetry (DSC) analyses were performed on a TA Instruments Discovery DSC using hermetically sealed aluminum Tzero pans. Scans were conducted under a nitrogen atmosphere at a heating and cooling rate of 10 °C/min unless otherwise noted. Thermogravimetric analyses (TGA) were performed on a TA Instruments Q500 under nitrogen atmosphere at a heating rate of 10 °C/min.

Synthesis

Catalyst Screening

Poly(butylene glycol succinate): (bio-PBGS). The catalysts were screened using the following protocol. An oven-dried, schlenk 100 mL round bottom flask equipped with a glass stir bar, was charged with succinic acid (4.40 g; 30 mmol) and (*R*)-(-)-1,3-butanediol (3.0 mL; 33 mmol). The

flask was fitted with a side-arm connector, a bump trap charged with $MgSO_{4\,(s)}$ (100 mg),[55] and a vacuum adapter with a collection flask to collect the distillate, shown in **Figure S1**. The assembled reaction vessel was evacuated and back filled with $N_{2(g)}$ (× 3) before being lowered into an aluminum heating block. Mechanical stirring was applied (500 rpm) as the block was slowly heated to 175 °C (2h). A steady flow of $N_{2(g)}$ was applied to promote the removal of water. Then, catalyst (500 ppm to total mol content) was added via a syringe. The catalysts $Ti(OBu)_4$ and $Sn(oct)_2$ were added via a hexanes stock solution. $Sb_2O_{3(s)}$ was insoluble and was added as a solid. All other catalysts were added via a toluene stock solution. After 30 min, the reaction vessel was placed under a dynamic vacuum (0.1 -0.3 atm) and slowly heated to 240 °C (2h). After cooling to room temperature, the polymer was dissolved in $CHCl_3$ (30 mL) and precipitated into cold MeOH (-40 °C; 250 mL × 2) then hexanes (25 °C; 100 mL). The resulting polymers were dried in a vacuum oven overnight (70 °C; 10-20h) to yield polyesters for NMR and SEC analysis.

Statistical Polymer Synthesis

Bio-Poly(butylene glycol succinate) (Bio-PBGS). Polycondensation reactions with diols and diacids were performed with the following method. (The reaction setup can be seen in **Figure S1**). The monomers, succinic acid (C4-diacid, 10.0 g; 85 mmol; 1.0 equi.) and (*R*)-(-)-1,3-butanediol (a.k.a. Bio-BG; 8.4 mL; 94 mmol; 1.1 equi.) were combined in an oven-dried, 100 mL, schlenk, round bottom flask equipped with a mechanical stirrer for overhead stirring. The reaction vessel was then evacuated and backfilled with $N_{2(g)}$ (× 3), before heating to 120 °C in an aluminum block under a steady, and low flow of $N_{2(g)}$. After 1h at 120 °C, the reaction temperature was slowly ramped up to 175 °C over the course of 2h to ensure full dehydration of the reaction. Then, titanium tetrabutoxide catalyst in hexanes (500 ppm to total mole content) was added via syringe. The

reaction was purged with $N_{2(g)}$ for an additional 30 min before the reaction vessel was then put under high vacuum (50-200 mTorr). The distillate was collected in an additional trap for analysis. The reaction was ramped to 200 °C over the course of 2 h, and stirred for an additional 2h, or until the melt viscosity plateaued according to the mechanical stirrer. The polymer cooled to room-temperature before dissolution in minimal CH_2Cl_2 (~15 mL) and precipitation into cold methanol (~300 mL; -40 °C × 2). The solution was decanted, and the polymer was dried in a vacuum over overnight (15h at 60-70 °C) to yield a colorless melt, 14.3 g (95%). M_n (THF SEC-MALLS) = 48,700 g/mol, Đ = 1.3, *dn/dc* = 0.0571. ^{1}H NMR (400 MHz, Chloroform-*d*) δ5.09 – 4.96 (m, 1H, BG-OC*H*-), 4.14 (t, *J* = 6.5 Hz, 2H, BG-OCH_2-), 2.61 (td, *J* = 3.9, 1.6 Hz, 4H, succinic-OOCCH_2CH_2COO-), 1.90 (dddd, *J* = 14.4, 12.3, 7.7, 3.4 Hz, 2H, BG-CH_2-), 1.27 (d, *J* = 6.3 Hz, 3H, BG-CH_3). ^{13}C NMR (101 MHz, $CDCl_3$) δ 172.17, 171.69, 68.28, 68.25, 61.04, 34.74, 29.35, 29.29, 29.05, 28.99, 20.02.

Bio-Poly(butylene glycol adipate) (Bio-PBGA). The biobased adipate derivative (C6-diacid) was prepared as previously described for Bio-PBGS with no changes to yield a clear colorless polymer melt, 6.7 g (87%). M_n (THF SEC-MALLS) = 34,700, Đ = 1.5, *dn/dc* = 0.0583. ^{1}H NMR (400 MHz, Chloroform-*d*) δ 5.08 – 4.95 (m, 1H, BG-OC*H*-), 4.18 – 4.06 (m, 2H, BG-OCH_2-), 2.32 (q, *J* = 6.9 Hz, 4H, adipic-OOCCH_2CH_2CH_2CH_2COO-), 1.99 – 1.79 (m, 2H, BG-CH_2-), 1.66 (p, *J* = 3.6 Hz, 4H, adipic-OOCCH_2CH_2CH_2CH_2COO-), 1.26 (d, *J* = 6.3 Hz, 3H, BG-CH_3). ^{13}C NMR (101 MHz, $CDCl_3$) δ 173.21, 172.75, 67.76, 60.70, 34.84, 34.13, 33.80, 24.39, 24.31, 20.10.

Bio-Poly(butylene glycol suberate) (Bio-PBGSu). The biobased suberate (C8-diacid) derivative was prepared as previously described for Bio-PBGS**,** except the initial dehydration was run overnight at 175 °C (12h) before the addition of catalyst and high vacuum to yield a colorless melt, 9.2 g (76%). M_n (THF SEC-MALLS) = 15,700, Đ = 1.3, *dn/dc* = 0.0599. ^{1}H NMR (400 MHz,

$CDCl_3$) ^{1}H NMR (400 MHz, Chloroform-*d*) δ 5.07 – 4.95 (m, 1H, BG-OC*H*-), 4.20 – 4.03 (m, 2H, BG-OCH_2-), 2.29 (td, *J* = 7.6, 6.4 Hz, 4H, suberic- OOCCH_2CH$_2$CH$_2$CH$_2$CH$_2$CH_2COO-), 2.04 – 1.77 (m, 2H, BG-CH_2-), 1.62 (tt, *J* = 7.4, 4.8 Hz, 4H, suberic-OOCCH$_2$CH_2CH$_2$CH$_2$CH_2CH$_2$COO-), 1.40 – 1.29 (m, 4H, suberic-OOCCH$_2$CH$_2$CH_2CH_2CH$_2$CH$_2$COO-), 1.26 (d, *J* = 6.3 Hz, 3H, BG-CH_3). ^{13}C NMR (101 MHz, $CDCl_3$) δ 173.60, 173.14, 67.62, 60.63, 34.86, 34.47, 34.14, 28.76, 24.78, 24.70, 20.11.

Bio-Poly(butylene glycol sebacate) (Bio-PBGSe). The biobased sebacate derivative was prepared as previously described for Bio-PBGS**,** except the initial dehydration was run overnight at 175 °C (14h) before the addition of catalyst to yield a colorless melt, 21.4 g (89%). M_n (THF SEC-MALLS) = 29,000, Đ = 1.3, *dn/dc* = 0.0606. ^{1}H NMR (400 MHz, Chloroform-*d*) δ 5.09 – 4.90 (m, 1H, BG-OC*H*-), 4.20 – 4.02 (m, 2H, BG-OCH_2-), 2.39 – 2.20 (m, 4H, sebacic-OOCCH_2CH$_2$CH$_2$CH$_2$CH$_2$CH$_2$CH_2COO-), 2.01 – 1.79 (m, 2H, BG-CH_2-), 1.61 (t, *J* = 7.3 Hz, 4H, sebacic-OOCCH$_2$CH_2CH$_2$CH$_2$CH$_2$CH$_2$CH_2CH$_2$COO-), 1.30 (s, 8H, sebacic-OOCCH$_2$CH$_2$CH_2CH_2CH_2CH_2CH$_2$CH$_2$COO-), 1.26 (d, *J* = 6.3 Hz, 3H, BG-CH_3). ^{13}C NMR (101 MHz, $CDCl_3$) δ 173.73, 173.26, 67.59, 60.62, 34.86, 34.56, 34.23, 29.09, 29.07, 24.96, 24.88, 20.12.

Bio-Poly(butylene glycol 1,14-tetradecanedioic acid) (Bio-PBGTD). The biobased 1,14-tetradecanedioic acid derivative was prepared as previously described for Bio-PBGSe to yield a white, fibrous solid, 7.1 g (95%). M_n (THF SEC-MALLS) = 49,700, Đ = 1.5, *dn/dc* = 0.0674. ^{1}H NMR (400 MHz, Chloroform-*d*) δ 5.09 – 4.97 (m, 1H, BG-OC*H*-), 4.19 – 4.05 (m, 2H, BG-OCH_2-), 2.34 – 2.24 (m, 4H, TD-OOCCH_2CH$_2$CH$_2$CH$_2$CH$_2$CH$_2$CH$_2$CH$_2$CH$_2$CH$_2$CH$_2$CH_2COO-), 1.99 – 1.80 (m, 2H, BG-CH_2-), 1.66 – 1.58 (m, 4H, TD-OOCCH$_2$CH_2CH$_2$CH$_2$CH$_2$CH$_2$CH$_2$CH$_2$CH$_2$CH$_2$CH_2CH$_2$COO-), 1.36 – 1.24 (m, 19H, TD-

OOCCH$_2$CH$_2$C*H$_2$*C*H$_2$*C*H$_2$*C*H$_2$*C*H$_2$*C*H$_2$*C*H$_2$*C*H$_2$*CH$_2$CH$_2$COO-, BG-C*H$_3$*). 13C NMR (101 MHz, CDCl3) δ 173.80, 173.33, 67.60, 60.62, 34.88, 34.61, 34.29, 29.60, 29.49, 29.29, 29.19, 29.16, 25.03, 24.94, 20.13.

Bio-Poly(butylene glycol 2,5-furandicarboxylate) (Bio-PBGF). The biobased furandicarboxylate derivative was prepared as previously described for Bio-PBGS, except five equivalences of bio-BG was used, and the titanium catalyst was present for the initial dehydration stage and run overnight at 175 °C (11h). After overnight at 175 °C, the temperature was ramped slowly to 240 °C over the course of 4 hours. The reaction was put under high vac (100 mTorr) for 0.5 hours before cooling to RT, and purification to yield a yellow solid, 5.8 g (80%). M_n (THF SEC-MALLS) = 15,100, Đ = 1.3, *dn/dc* = 0.1110. ^{1}H NMR (400 MHz, Chloroform-*d*) δ 7.18 (s, 2H), 5.39 – 5.29 (m, 1H), 4.53 – 4.38 (m, 2H), 2.29 – 2.07 (m, 2H), 1.45 (d, *J* = 6.3 Hz, 3H). ^{13}C NMR (101 MHz, $CDCl_3$) δ 157.81, 157.78, 157.52, 157.48, 146.98, 146.88, 146.64, 146.54, 118.59, 118.44, 77.36, 77.04, 76.72, 69.66, 61.82, 34.73, 20.17

Bio-Poly(butylene glycol terephthalate) (Bio-PBGT). The bio-PBGT polymer was prepared in two steps. First, the terephthalate diester was prepared from terephthaloyl chloride and bio-BG, followed by polycondensation. The bis-bio-butylene glycol terephthalate pre-polymer (*bis*-bio-BGT) was prepared via substitution (**Scheme 3**). The diol, (*R*)-(-)-1,3-butanediol (13.3 mL, 150 mmol; 3.0 equi.), triethylamine (15.3 mL, 110 mmol; 2.1 equi.), and $CH_2Cl_{2(anhydrous)}$ (130 mL) were combined into a 3-neck, 500 mL round bottom flask and chilled to -15 °C (conc. $NaCl_{(aq)}$/ H_2O/ ice). The reaction vessel was fitted with an addition funnel (100 mL) with terephthaloyl chloride (10.0 g, 50 mmol, 1.0 equi.) dissolved in $CH_2Cl_{2(anhydrous)}$ (~85 mL). The terephthaloyl chloride/CH_2Cl_2 solution was added dropwise over the course of 3h. The reaction was stirred overnight (14h), before adding 1.0 M $HCl_{(aq)}$ (100 mL). The reaction contents were added to a

separation funnel to isolate the organic layer (CH_2Cl_2) and was washed with 1.0 M $HCl_{(aq)}$ (100 mL × 4), discarding the aqueous layer each time. The organic layer was washed with water (100 mL × 2) and brine (100 mL × 2) before drying over $MgSO_{4(s)}$ (~5 g). The organic layer was filtered, reduced via rotary evaporation yielding a yellow semi-solid after left standing for 2h. The product was recrystallized (acetone/hexanes) to yield a white powder, 10.01 g (66% yield; >99% regioregular; **Figure S42**). ^{1}H NMR (400 MHz, Chloroform-*d*) δ 8.09 (s, 4H, Ar*H*), 4.60 (ddd, *J* = 11.2, 8.4, 5.4 Hz, 2H, $HOCH_3CHCH_2CH_2OOC$-Ar-$COOCH_2CH_2CHCH_3OH$), 4.44 (dt, *J* = 11.3, 5.7 Hz, 2H, $HOCH_3CHCH_2CH_2OOC$-Ar-$COOCH_2CH_2CHCH_3OH$), 4.00 (dqd, *J* = 8.5, 6.2, 4.0 Hz, 2H, $HOCH_3CHCH_2CH_2OOC$-Ar-$COOCH_2CH_2CHCH_3OH$), 2.04 – 1.79 (m, 4H, $HOCH_3CHCH_2CH_2OOC$-Ar-$COOCH_2CH_2CHCH_3OH$), 1.29 (d, *J* = 6.2 Hz, 6H, $HOCH_3CHCH_2CH_2OOC$-Ar-$COOCH_2CH_2CHCH_3OH$). ^{13}C NMR (101 MHz, $CDCl_3$) δ 166.08, 134.00, 129.58, 64.80, 62.65, 38.07, 23.65. HRMS (ESI) Calc for $C_{16}H_{22}O_6Na$ $[M+Na]^+$ = 333.1314, found 333.1312. The *bis*-bio-BGT was then polymerized as previously described for bio-PBGF without addition of bio-BG and purified to yield a white, fluffy solid, 5.8 g (80%). M_n (THF SEC-MALLS) = 21,600, Đ = 1.7, *dn/dc* = 0.1350. ^{1}H NMR (400 MHz, Chloroform-*d*) δ 8.06 (tt, *J* = 5.7, 2.0 Hz, 4H, 2,3,5,6-Ar*H*), 5.50 – 5.36 (m, 1H), 4.49 (dddd, *J* = 27.7, 13.4, 6.5, 4.1 Hz, 2H), 2.37 – 2.06 (m, 2H), 1.48 (d, *J* = 6.3 Hz, 3H). ^{13}C NMR (101 MHz, $CDCl_3$) δ 165.62, 165.60, 165.17, 165.15, 134.23, 134.19, 133.86, 133.82, 129.52, 69.29, 61.81, 53.43, 34.97, 20.24.

Reference Polymers

Poly(2-methyl,1,3-propylene succinate) P2MPS. The regio-chemical reference succinate polymer was prepared as previously described for bio-PBGS**,** except 2-methyl 1,3-propanediol was used in place of (*R*)-(-)-1,3-butanediol to yield a colorless polymer melt, 10.5 g (77%). M_n (THF SEC-MALLS) = 47,400, Đ = 1.5, *dn/dc* = 0.0566; ^{1}H NMR (400 MHz, Chloroform-*d*) δ 4.19 – 3.93

(m, 4H, diol- OCH_2CHCH$_3$CH_2O-), 2.64 (s, 4H, succinate-COCH_2CH_2CO-), 2.27 – 2.08 (m, J = 6.5 Hz, 1H, diol- OCH$_2$CHCH$_3$CH$_2$O), 0.99 (d, J = 6.9 Hz, 3H, diol-OCH$_2$CHCH_3CH$_2$O). ^{13}C NMR (101 MHz, $CDCl_3$) δ 172.14, 66.01, 32.39, 28.96, 13.78.

Poly(propylene succinate) PPS. The unsubstituted reference succinate polymer was prepared as previously described for bio-PBGS**,** 1,3-propanediol was used in place of (*R*)-(-)-1,3-butanediol to yield an opaque solid, 15.0 g (97%). M_n (THF SEC-MALLS) = 48,300, Đ = 1.8, *dn/dc* = 0.0654*;* ^{1}H NMR (400 MHz, Chloroform-*d*) δ 4.18 (t, J = 6.3 Hz, 4H, diol- OCH_2CH$_2$CH_2O-), 2.63 (s, 4H, succinate-COCH_2CH_2CO-), 1.98 (p, J = 6.3 Hz, 2H, - OCH$_2$CH_2CH$_2$O-). ^{13}C NMR (101 MHz, $CDCl_3$) δ 172.17, 61.27, 28.96, 27.89.

Poly(butylene succinate) PBS. The unsubstituted reference succinate polymer was prepared as previously described for bio-PBGS**,** 1,4-butanediol was used in place of (*R*)-(-)-1,3-butanediol to yield a white solid. 17.0 g (92%). M_n ($CHCl_3$ SEC-vs. PS standards) = 62,000, Đ =2.4. ^{1}H NMR (400 MHz, Chloroform-d) δ 4.25 – 3.97 (m, 4H, diol-OCH_2CH$_2$CH$_2$CH_2O-), 2.62 (s, 4H, succinate-COCH_2CH_2CO-), 1.78 – 1.61 (m, 4H, diol-OCH$_2$CH_2CH_2CH$_2$O-). ^{13}C NMR (101 MHz, $CDCl_3$) δ 172.28, 64.16, 29.02, 25.21

Oligomer Synthesis

Bio-Oligo(butylene glycol succinate) (Bio-OBGS). A low molar mass polymer between succinic acid and (*R*)-(-)-1,3-butanediol was prepared using the following method. Succinic acid (8.9 g, 75 mmol;1 equivalence) and bio-BG (7.42 mL; 82 mmol; 1.1 equivalence) were combined in a 50 mL round bottom schlenk flask with a Teflon-coated stir bar. The reaction flask was fitted with a Dean-stark trap apparatus, a condenser, and a drying tube with $CaCl_{2(s)}$ before being heated to 140 °C overnight (16h). A constant, slow stream of $N_{2(g)}$ was applied the reaction overnight to facilitate

evaporation. After the theoretical amount of water collected in the trap (~2.7 mL), the reaction temperature was elevated to 180 °C and put under dynamic vacuum for an additional 2h to remove residual bio-BG. The product was cooled to RT before being collected and used without further purification as a colorless polymer melt, 12.4 g (96%). M_n (SEC-vs. PS standards) =1,700 g/mol, Đ = 1.8; ^{1}H NMR (400 MHz, Chloroform-*d*) δ 5.01 – 4.89 (m, 23H), 4.26 (ddd, *J* = 11.2, 8.2, 5.6 Hz, 2H), 4.07 (t, *J* = 6.5 Hz, 46H), 3.95 – 3.78 (m, 1H), 3.57 (h, *J* = 5.4 Hz, 1H), 2.64 – 2.49 (m, 104H), 1.92 – 1.73 (m, 48H), 1.19 (d, *J* = 6.3 Hz, 75H). ^{13}C NMR (101 MHz, $CDCl_3$) δ 175.82, 172.52, 172.45, 172.21, 172.14, 172.08, 171.73, 171.67, 68.63, 68.22, 68.20, 64.64, 61.95, 60.98, 58.57, 38.80, 37.79, 34.65, 29.28, 29.23, 29.18, 29.09, 28.99, 28.93, 28.89, 28.76, 28.68, 23.35, 20.29, 19.96.

Regioregular Polymer Synthesis

Ethyl 4-hydroxybenzoate. The ethyl ester of 4-hydroxybenzoic acid was prepared as previously described by Ito and coworkers with the following changes.[86] The reaction mixture was precipitated into a $NaHCO_{3(s)}$/ ice water slurry, filtered through a coarse frit, washed with copious amounts of sat. $NaHCO_{3(aq)}$ and recrystallized with acetone to yield a white crystalline solid, 26.0 g (43%). ^{1}H NMR spectra are in accordance with literature values.[86]

(R)-3-hydroxybutyl 4-methyl benzenesulfonate (*R*-TsBG). The tosyl-bio-BG compound was prepared by regioselective tosylation of Bio-BG as previously described by Steinmetz and coworkers with the following changes.[87] The product was isolated by extraction and not purified further by column chromatography. The product was acquired as a colorless oil, 53 g (85% yield; 92% regioregular; **Figure S52**). ^{1}H NMR spectra are in accordance with literature values.[19]

3-hydroxybutyl 4-methyl benzenesulfonate (*rac*-TsBG). The tosylated racemic-BG was prepared as previously described with no changes.[87] ^{1}H NMR spectra are in accordance with literature values.[86]

Ethyl (R)-4-(3-hydroxybutoxy)benzoate (*R*-BGBz). The regio-enriched aromatic monomer was prepared by Williamson ether synthesis.[88] The reagents, ethyl 4-hydroxybenzoate (10.0 g, 60 mmol), TsBG (12.2 g, 50 mmol) $K_2CO_{3(s)}$ (25 g, 181 mmol) and lithium bromide (LiBr; 500 mg, 5.7 mmol), were combined in a 250 mL round bottom flask before dissolution in DMF (75 mL). The reaction flask was then fitted with a reflux condenser before the reaction mixture was heated to 60 °C. The reaction was monitored by thin later chromatography until complete consumption of the TsBG (limiting reagent; R_f = 0.23 in 1:1 hexanes/EtOAc; consumed in ~2.5h). Then, the reaction mixture was filtered to remove the potassium carbonate solid and washed with EtOAc. Distilled water (~250 mL) was added to the reaction mixture before extraction with a separation funnel with EtOAc (150 mL × 2). The organic layer was washed with 1.0 M NaOH (150 mL × 2) to remove the phenol starting material, followed by washing with H_2O (150 mL × 4) to remove the DMF, and then brine (150 mL × 2). The organic layer was dried over $MgSO_{(s)}$ (~5 g) and filtered before removing the solvent via rotary evaporation to yield a colorless oil. Upon resting overnight (10h) the colorless oil solidified. The solid residue was recrystallized via acetone/hexanes (~1:1), filtered, then recrystallized from diethyl ether to yield a white, crystalline solid (5.87 g; 49 % yield). ^{1}H NMR (400 MHz, Chloroform-*d*) δ 8.00 (d, *J* = 8.9 Hz, 2H, 2,6-Ar*H*), 6.93 (d, *J* = 8.9 Hz, 2H, 3,5-Ar*H*), 4.36 (q, *J* = 7.1 Hz, 2H, ArCOO-C*H*$_2$CH$_3$), 4.26 – 4.07 (m, 3H, BG-C*H*-, BG-OC*H*$_2$-), 2.01 – 1.90 (m, 3H, BG-O*H*, BG-C*H*$_2$), 1.39 (t, *J* = 7.1 Hz, 3H, ArCOO-CH$_2$C*H*$_3$), 1.30 (d, *J* = 6.2 Hz, 3H, BG-C*H*$_3$). ^{13}C NMR (101 MHz, $CDCl_3$) δ 166.41, 162.48,

131.56, 123.04, 114.03, 65.72, 60.67, 38.06, 23.82, 14.38. HRMS (ESI) Calc for $C_{13}H_{18}O_4Na$ $[M+Na]^+$ = 261.1103, found 261.1174.

Ethyl, 4-(3-hydroxybutoxy)benzoate (rac-BGBz). The racemic regio-enriched aromatic monomer was prepared by Williamson ether synthesis as previously described for R-BGBz with the following changes. After the extraction, a colorless oil as isolated. The product was purifed via gradient column chromatography (5:1 EtOAc/ hexanes to 1:1 EtOac/hexanes) followed by recrystallization from diethyl ether to yield a white powder (3.1 g; 23%). ^{1}H NMR (400 MHz, Chloroform-d) δ 7.98 (d, J = 8.9 Hz, 1H), 6.91 (d, J = 8.9 Hz, 1H), 4.34 (q, J = 7.1 Hz, 1H), 4.28 – 4.00 (m, 2H), 2.24 (s, 1H), 2.01 – 1.85 (m, 1H), 1.38 (t, J = 7.1 Hz, 2H), 1.28 (d, J = 6.2 Hz, 2H). ^{13}C NMR (101 MHz, CDCl3) δ 166.43, 162.51, 131.54, 122.96, 114.03, 65.67, 65.55, 60.67, 38.07, 23.80, 14.36. HRMS (ESI) Calc for $C_{13}H_{18}O_4Na$ $[M+Na]^+$ = 261.1103, found 261.1164.

Poly((R)-4-(3-hydroxybutoxy)benzoate) (*R*-PBGBz). The regioregular polymer was prepared via step-growth homopolymerization. The monomer (R-BGBz; 1.30 g, 5.5 mmol) was weighed into a 10 mL, two neck round-bottom flask. The round-bottom flask was fitted with a bump-trap and a $N_{2(g)}$ inlet before submerging into a sand bath. The reaction vessel was evacuated and back-filled with $N_{2(g)}$ (× 4) before heating to 100 °C. After 30 min at 100 °C , the catalyst ($TiOBu_4$) in hexanes was added via syringe (17 mg; 0.275 mmol). The reaction mixture was heated to 150 °C (2h), 170 °C (2h), and 180 °C overnight (10h) under a low nitrogen flow. Finally, the reaction mixture was heated to 245 °C under high vacuum (100 mTorr) for 5h. The reaction cooled to RT under $N_{2(g)}$ and dissolved in $CHCl_3$/TFA (~1:1), precipitated into cold MeOH (-40 °C) collected by filtration and dried to yield a white solid (1.04 g; 96% yield). ^{1}H NMR (400 MHz, TFA-*d*, Chloroform-*d*) δ 7.97 (d, *J* = 8.9 Hz, 2H, 2,6-Ar*H*), 6.94 (d, *J* = 8.9 Hz, 2H, 3,5-Ar*H*), 5.53 – 5.38 (m, 1H, BG-C*H*-), 4.20 (td, *J* = 6.0, 2.1 Hz, 2H, BG-OCH_2-), 2.38 – 2.16 (m, 2H, BG-CH_2), 1.49 (d, *J* = 6.3 Hz,

3H, BG-CH_3). ^{13}C NMR (101 MHz, TFA-*d*, $CDCl_3$) δ 169.25, 163.24, 131.94, 121.55, 114.40, 70.78, 64.57, 35.08, 19.51.

Ethyl, 4-(3-hydroxybutoxy)benzoate (rac-PBGBz).The racemic regioregular polymer was prepared as previously described for PR-BGBz, but the monomer rac-BGBz was used in place of R-BGBz. The polymer was purified by dissolution in $CHCl_3$/TFA and precipitation into cold MeOH (-40 °C). The product was collected by filtration and dried to yield a white solid (502 mg; 81% yield). (400 MHz, Chloroform-*d*) δ 8.04 – 7.88 (m, 2H), 7.00 – 6.77 (m, 2H), 5.46 – 5.34 (m, 1H), 4.13 (t, J = 6.3 Hz, 2H), 2.40 – 2.07 (m, 2H), 1.52 – 1.36 (m, 3H). ^{13}C NMR (101 MHz, CDCl3) δ 165.90, 162.58, 131.56, 122.85, 114.09, 68.52, 64.67, 35.60, 20.42.

ASSOCIATED CONTENT

See Supporting information for images of the polymerization setup (**Figure S1**), data from the catalyst screening (**Figures S2-S3**), temperature-dependent kinetics data (**Figures S4-S7**), 1D and 2D-NMR spectra of bio-OBGS (**Figures S8-S11**), data for bio-PBGF (**Table S1** and **Figure S12**), reference tables comparing polymer thermal properties (**Table S2-S4**), SEC plots (**Figures S13-S29**), ^{1}H and ^{13}C NMR spectroscopy of biobased monomers and polymers (**Figures S30-S60**), and HRMS data (**Figures S61-S64**). This material is available free of charge via the internet at http://pubs.acs.org.

DATA ACCESS STATEMENT

Primary data files (NMR spectroscopy, DSC, TGA, and SEC) are available free of charge at https://doi.org/10.13020/7fkh-c288.

Corresponding Author

E-mail: hillmyer@umn.edu (M. A. H.)

ORCID:

Marc A. Hillmyer: 0000-0001-8255-3853

Frank S. Bates: 0000-0003-3977-1278

ACKNOWLEDGMENT

We thank Genomatica for supplying the enantiomerically pure (*R*)-(-)-1,3-butanediol and financial support for this work. We thank Fasil Tadesse, Juila Khandurina and Jeff Lievense at Genomatica for helpful discussions. We would like to thank John Beumer for assistance creating the TOC graphic. We thank members of the National Science Foundation's Center for Sustainable Polymers for helpful discussions and insights. We thank Esra Altay, Lucie Fournier, Yoon-Jung Jang, and Huiqun Wang at the University of Minnesota for assistance with instrumentation and helpful discussions.

REFERENCES

(1) Schneiderman, D. K.; Hillmyer, M. A. 50th Anniversary Perspective: There Is a Great Future in Sustainable Polymers. *Macromolecules* **2017**, *50*, 3733–3749. https://doi.org/10.1021/acs.macromol.7b00293.

(2) Geyer, R.; Jambeck, J. R.; Law, K. L. Production, Use, and Fate of All Plastics Ever Made. *Sci. Adv.* **2017**, *3*, e1700782. https://doi.org/10.1126/sciadv.1700782.

(3) Hillmyer, M. A. The Promise of Plastics from Plants. *Science* **2016**, *352*, 1392–1393. https://doi.org/10.1126/science.aao6711.

(4) MacArthur, D. E. Beyond Plastic Waste. *Science* **2017**, *358*, 843.

https://doi.org/10.1126/science.aao6749.

(5) Albertsson, A. C.; Hakkarainen, M. Designed to Degrade. *Science* **2017**, *358*, 872–873. https://doi.org/10.1126/science.aap8115.

(6) Vilela, C.; Sousa, A. F.; Fonseca, A. C.; Serra, A. C.; Coelho, J. F. J.; Freire, C. S. R.; Silvestre, A. J. D. The Quest for Sustainable Polyesters-Insights into the Future. *Polym. Chem.* **2014**, *5*, 3119–3141. https://doi.org/10.1039/c3py01213a.

(7) Garcia, J. M.; Robertson, M. L. The Future of Plastics Recycling. *Science* **2017**, *358*, 870–872. https://doi.org/10.1126/science.aaq0324.

(8) Rasal, R. M.; Janorkar, A. V.; Hirt, D. E. Poly(Lactic Acid) Modifications. *Prog. Polym. Sci.* **2010**, *35*, 338–356. https://doi.org/10.1016/j.progpolymsci.2009.12.003.

(9) Madhavan Nampoothiri, K.; Nair, N. R.; John, R. P. An Overview of the Recent Developments in Polylactide (PLA) Research. *Bioresour. Technol.* **2010**, *101*, 8493–8501. https://doi.org/10.1016/j.biortech.2010.05.092.

(10) Scheirs, J.; Long, T. E. *Modern Polyesters: Chemistry and Technology of Polyesters and Copolyesters*; 2004. https://doi.org/10.1002/0470090685.

(11) Tong, R. New Chemistry in Functional Aliphatic Polyesters. *Ind. Eng. Chem. Res.* **2017**, *56*, 4207–4219. https://doi.org/10.1021/acs.iecr.7b00524.

(12) Wilfong, R. E. Linear Polyesters. *J. Polym. Sci.* **1961**, *54*, 385–410. https://doi.org/10.1002/pol.1961.1205416010.

(13) Auras, R.; Singh, S.; Singh, J. Performance Evaluation of PLA against Existing PET and PS Containers. *J. Test. Eval.* **2006**, *34*, 100041. https://doi.org/10.1520/jte100041.

(14) Japu, C.; Martínez De Ilarduya, A.; Alla, A.; García-Martín, M. G.; Galbis, J. A.; Muñoz-Guerra, S. Bio-Based PBT Copolyesters Derived from d-Glucose: Influence of Composition

on Properties. *Polym. Chem.* **2014**, *5*, 3190–3202. https://doi.org/10.1039/c3py01425h.

(15) Hocking, M. B. Commercial Polycondensation (Step-Growth) Polymers. In *Handbook of Chemical Technology and Pollution Control*; 2005. https://doi.org/10.1016/b978-012088796-5/50024-7.

(16) Zeng, J.-B. B.; Huang, C.-L. L.; Jiao, L.; Lu, X.; Wang, Y.-Z. Z.; Wang, X.-L. L. Synthesis and Properties of Biodegradable Poly(Butylene Succinate-Co-Diethylene Glycol Succinate) Copolymers. *Ind. Eng. Chem. Res.* **2012**, *51*, 12258–12265. https://doi.org/10.1021/ie300133a.

(17) Garcia, J. J.; Miller, S. A. Polyoxalates from Biorenewable Diols via Oxalate Metathesis Polymerization. *Polym. Chem.* **2014**, *5*, 955–961. https://doi.org/10.1039/c3py01185b.

(18) Short, G. N.; Nguyen, H. T. H.; Scheurle, P. I.; Miller, S. A. Aromatic Polyesters from Biosuccinic Acid. *Polym. Chem.* **2018**, *9*, 4113–4119. https://doi.org/10.1039/c8py00862k.

(19) Pang, C.; Jiang, X.; Yu, Y.; Chen, L.; Ma, J.; Gao, H. Copolymerization of Natural Camphor-Derived Rigid Diol with Various Dicarboxylic Acids: Access to Biobased Polyesters with Various Properties. *ACS Macro Lett.* **2019**, 1442–1448. https://doi.org/10.1021/acsmacrolett.9b00570.

(20) Nsengiyumva, O.; Miller, S. A. Synthesis, Characterization, and Water-Degradation of Biorenewable Polyesters Derived from Natural Camphoric Acid. *Green Chem.* **2019**, *21*, 973–978. https://doi.org/10.1039/C8GC03990A.

(21) Li, C.; Sablong, R. J.; Koning, C. E. Chemoselective Alternating Copolymerization of Limonene Dioxide and Carbon Dioxide: A New Highly Functional Aliphatic Epoxy Polycarbonate. *Angew. Chem. - Int. Ed.* **2016**, *55*, 11572–11576. https://doi.org/10.1002/anie.201604674.

(22) Thomsett, M. R.; Moore, J. C.; Buchard, A.; Stockman, R. A.; Howdle, S. M. New Renewably-Sourced Polyesters from Limonene-Derived Monomers. *Green Chem.* **2019**, *21*, 149–156. https://doi.org/10.1039/c8gc02957a.

(23) Hillmyer, M. A.; Tolman, W. B. Aliphatic Polyester Block Polymers: Renewable, Degradable, and Sustainable. *Acc. Chem. Res.* **2014**, *47*, 2390–2396. https://doi.org/10.1021/ar500121d.

(24) Zhang, D.; Hillmyer, M. A.; Tolman, W. B. Catalytic Polymerization of a Cyclic Ester Derived from a "Cool" Natural Precursor. *Biomacromolecules* **2005**, *6*, 2091–2095. https://doi.org/10.1021/bm050076t.

(25) Kimura, Y. Molecular, Structural, and Material Design of Bio-Based Polymers. *Polym. J.* **2009**, *41*, 797–807. https://doi.org/10.1295/polymj.PJ2009154.

(26) Overberger, C. G.; Parker, G. M. Optically Active Polyamides, Polymers from α-, β-, γ-, and ϵ-Methyl-ϵ-Caprolactam. *J. Polym. Sci. Part C Polym. Symp.* **2007**, *22*, 387–406. https://doi.org/10.1002/polc.5070220132.

(27) Mochizuki, M.; Hirami, M. Structural Effects on Biodegradation of Aliphatic Polyesters. *Polym. Adv. Technol.* **1997**, *8*, 203–209. https://doi.org/10.1002/(SICI)1099-1581(199704)8:4<203::AID-PAT627>3.0.CO;2-3.

(28) Zhang, C.; Schneiderman, D. K.; Cai, T.; Tai, Y.-S.; Fox, K.; Zhang, K. Optically Active β-Methyl-δ-Valerolactone: Biosynthesis and Polymerization. *ACS Sustain. Chem. Eng.* **2016**, *4*, 4396–4402. https://doi.org/10.1021/acssuschemeng.6b00992.

(29) Grenier, D.; Prud'homme, R. E. Complex Formation between Enantiomeric Polyesters. *J. Polym. Sci. Polym. Phys. Ed.* **1984**, *22*, 577–587. https://doi.org/10.1002/pol.1984.180220404.

(30) Testud, B.; Pintori, D.; Grau, E.; Taton, D.; Cramail, H. Hyperbranched Polyesters by Polycondensation of Fatty Acid-Based AB : N -Type Monomers. *Green Chem*. **2017**, *19*, 259–269. https://doi.org/10.1039/c6gc02294d.

(31) Dirlam, P. T.; Goldfeld, D. J.; Dykes, D. C.; Hillmyer, M. A. Polylactide Foams with Tunable Mechanical Properties and Wettability Using a Star Polymer Architecture and a Mixture of Surfactants. *ACS Sustain. Chem. Eng*. **2019**, *7*, 1698–1706. https://doi.org/10.1021/acssuschemeng.8b05461.

(32) Miller, S. A. Sustainable Polymers: Opportunities for the next Decade. *ACS Macro Lett*. **2013**, *2*, 550–554. https://doi.org/10.1021/mz400207g.

(33) Aeschelmann, F.; Carus, M. Biobased Building Blocks and Polymers in the World: Capacities, Production, and Applications–Status Quo and Trends Towards 2020. *Ind. Biotechnol*. **2015**, *11*, 154–159. https://doi.org/10.1089/ind.2015.28999.fae.

(34) Burgard, A.; Burk, M. J.; Osterhout, R.; Van Dien, S.; Yim, H. Development of a Commercial Scale Process for Production of 1,4-Butanediol from Sugar. *Curr. Opin. Biotechnol*. **2016**, *42*, 118–125. https://doi.org/10.1016/j.copbio.2016.04.016.

(35) Nishiguchi, K.; Himeji-shi, H. An Improved Process for the Preparation of 1,3-Butylene Glycol. DE69328043D1, 1998.

(36) Jira, R. Acetaldehyde from Ethylene - A Retrospective on the Discovery of the Wacker Process. *Angew. Chem. - Int. Ed*. **2009**, *48*, 9034–9037. https://doi.org/10.1002/anie.200903992.

(37) Olah, G. A.; Goeppert, A.; Prakash, G. K. S. Methanol-Based Chemicals, Synthetic Hydrocarbons, and Materials. In *Beyond Oil and Gas*; 2018. https://doi.org/10.1002/9783527805662.ch14.

(38) Kimmerer, T. W.; Kozlowski, T. T. Ethylene, Ethane, Acetaldehyde, and Ethanol Production By Plants under Stress. *Plant Physiol.* **1982**, *69*, 840–847. https://doi.org/10.1104/pp.69.4.840.

(39) Pacheco, R.; Huston, K. Life Cycle Assessment (LCA) of Naturally-Sourced and Petroleum-Based Glycols Commonly Used in Personal Care Products Life Cycle Assessment (LCA) of Naturally-Sourced and Petroleum-Based Glycols Commonly Used in Personal Care Products. *SOFW J.* **2018**, *144*, 11–15.

(40) Tabone, M. D.; Cregg, J. J.; Beckman, E. J.; Landis, A. E. Sustainability Metrics: Life Cycle Assessment and Green Design in Polymers. *Environ. Sci. Technol.* **2010**, *44*, 8264–8269. https://doi.org/10.1021/es101640n.

(41) García-Bernabé, A.; Díaz Calleja, R.; Sanchis, M. J.; Del Campo, A.; Bello, A.; Pérez, E. Amorphous-Smectic Glassy Main Chain LCPs. II. Dielectric Study of the Glass Transition. *Polymer (Guildf).* **2004**, *45*, 1533–1543. https://doi.org/10.1016/j.polymer.2003.12.073.

(42) Del Campo, A.; Bello, A.; Pérez, E.; García-Bernabé, A.; Díaz Calleja, R. Amorphous-Smectic Glassy Main-Chain LCPs, 1: Poly(Ether Esters) Derived from Hydroxybibenzoic Acid and (R,S)- and (R)-2-Methylpropane-1,3-Diol. *Macromol. Chem. Phys.* **2002**, *203*, 2508–2515. https://doi.org/10.1002/macp.200290028.

(43) Fernández-Blázquez, J. P.; Bello, A.; Pérez, E. Observation of Two Glass Transitions in a Thermotropic Liquid-Crystalline Polymer. *Macromolecules* **2004**, *37*, 9018–9026. https://doi.org/10.1021/ma049354r.

(44) Tsutsumi, C.; Yasuda, H. Biodegradation of Copolymers Composed of Optically ActiveL-Lactide and (R)- or (S)-1-Methyltrimethylene Carbonate. *J. Polym. Sci. Part A Polym. Chem.* **2001**, *39*, 3916–3927. https://doi.org/10.1002/pola.10035.

(45) Yasuda, H.; Aludin, M.-S.; Kitamura, N.; Tanabe, M.; Sirahama, H. Syntheses and Physical Properties of Novel Optically Active Poly(Ester-Carbonate)s by Copolymerization of Substituted Trimethylene Carbonate with ε-Caprolactone and Their Biodegradation Behavior. *Macromolecules* **1999**, *32*, 6047–6057. https://doi.org/10.1021/ma981904w.

(46) Nishiwaki, Y.; Kimura, Y.; Masutani, K.; Lee, C. W. High-Molecular-Weight Poly(1,2-Propylene Succinate): A Soft Biobased Polyester Applicable as an Effective Modifier of Poly(l-Lactide). *J. Polym. Sci. Part A Polym. Chem.* **2018**, *56*, 1795–1805. https://doi.org/10.1002/pola.29060.

(47) Lei, L.; Ding, T.; Shi, R.; Liu, Q.; Zhang, L.; Chen, D.; Tian, W. Synthesis, Characterization and in Vitro Degradation of a Novel Degradable Poly((1,2-Propanediol-Sebacate)-Citrate) Bioelastomer. *Polym. Degrad. Stab.* **2007**, *92*, 389–396. https://doi.org/10.1016/j.polymdegradstab.2006.12.004.

(48) Stadler, B. M.; Brandt, A.; Kux, A.; Beck, H.; de Vries, J. G. Properties of Novel Polyesters Made from Renewable 1,4-Pentanediol. *ChemSusChem* **2019**, *13*, 556–563. https://doi.org/10.1002/cssc.201902988.

(49) Lutz, J. F. Coding Macromolecules: Inputting Information in Polymers Using Monomer-Based Alphabets. *Macromolecules* **2015**, *48*, 4759–4767. https://doi.org/10.1021/acs.macromol.5b00890.

(50) Lutz, J.-F. Aperiodic Copolymers. *ACS Macro Lett.* **2014**, *3*, 1020–1023. https://doi.org/10.1021/mz5004823.

(51) Stille, J. K. Step-Growth Polymerization. *J. Chem. Educ.* **1981**, *58*, 862. https://doi.org/10.1021/ed058p862.

(52) Edlund, U.; Albertsson, A. C. Polyesters Based on Diacid Monomers. *Adv. Drug Deliv. Rev.*

2003, *55*, 585–609. https://doi.org/10.1016/S0169-409X(03)00036-X.

(53) Amador, A. G.; Watts, A.; Neitzel, A. E.; Hillmyer, M. A. Entropically Driven Macrolide Polymerizations for the Synthesis of Aliphatic Polyester Copolymers Using Titanium Isopropoxide. *Macromolecules* **2019**, *52*, 2371–2383. https://doi.org/10.1021/acs.macromol.9b00065.

(54) Jacquel, N.; Freyermouth, F.; Fenouillot, F.; Rousseau, A.; Pascault, J. P.; Fuertes, P.; Saint-Loup, R. Synthesis and Properties of Poly(Butylene Succinate): Efficiency of Different Transesterification Catalysts. *J. Polym. Sci. Part A Polym. Chem.* **2011**, *49*, 5301–5312. https://doi.org/10.1002/pola.25009.

(55) Qi, P.; Chen, H. L.; Nguyen, H. T. H.; Lin, C. C.; Miller, S. A. Synthesis of Biorenewable and Water-Degradable Polylactam Esters from Itaconic Acid. *Green Chem.* **2016**, *18*, 4170–4175. https://doi.org/10.1039/c6gc01081d.

(56) Stempfle, F.; Ortmann, P.; Mecking, S.; Stemp, F.; Ortmann, P.; Mecking, S. Long-Chain Aliphatic Polymers to Bridge the Gap between Semicrystalline Polyolefins and Traditional Polycondensates. *Chem. Rev.* **2016**, *116*, 4597–4641. https://doi.org/10.1021/acs.chemrev.5b00705.

(57) Debuissy, T.; Pollet, E.; Avérous, L. Synthesis of Potentially Biobased Copolyesters Based on Adipic Acid and Butanediols: Kinetic Study between 1,4- and 2,3-Butanediol and Their Influence on Crystallization and Thermal Properties. *Polymer*. **2016**, *99*, 204–213. https://doi.org/10.1016/j.polymer.2016.07.022.

(58) Wang, J.; Sun, L.; Shen, Z.; Zhu, J.; Song, X.; Liu, X. Effects of Various 1,3-Propanediols on the Properties of Poly(Propylene Furandicarboxylate). *ACS Sustain. Chem. Eng.* **2019**, *7*, 3282–3291. https://doi.org/10.1021/acssuschemeng.8b05288.

(59) Pang, C.; Jiang, X.; Yu, Y.; Liu, X.; Lian, J.; Ma, J.; Gao, H. Sustainable Polycarbonates from a Citric Acid-Based Rigid Diol and Recycled BPA-PC: From Synthesis to Properties. *ACS Sustain. Chem. Eng.* **2018**, *6*, 17059–17067. https://doi.org/10.1021/acssuschemeng.8b04421.

(60) Ma, C.; Xu, F.; Cheng, W.; Tan, X.; Su, Q.; Zhang, S. Tailoring Molecular Weight of Bioderived Polycarbonates via Bifunctional Ionic Liquids Catalysts under Metal-Free Conditions. *ACS Sustain. Chem. Eng.* **2018**, *6*, 2684–2693. https://doi.org/10.1021/acssuschemeng.7b04284.

(61) Watts, A.; Kurokawa, N.; Hillmyer, M. A. Strong, Resilient, and Sustainable Aliphatic Polyester Thermoplastic Elastomers. *Biomacromolecules* **2017**, *18*, 1845–1854. https://doi.org/10.1021/acs.biomac.7b00283.

(62) Wilbon, P. A.; Swartz, J. L.; Meltzer, N. R.; Brutman, J. P.; Hillmyer, M. A.; Wissinger, J. E. Degradable Thermosets Derived from an Isosorbide/Succinic Anhydride Monomer and Glycerol. *ACS Sustain. Chem. Eng.* **2017**, *5*, 9185–9190. https://doi.org/10.1021/acssuschemeng.7b02096.

(63) van der Klis, F.; Knoop, R. J. I.; Bitter, J. H.; van den Broek, L. A. M. The Effect of Me-Substituents of 1,4-Butanediol Analogues on the Thermal Properties of Biobased Polyesters. *J. Polym. Sci. Part A Polym. Chem.* **2018**, *56*, 1903–1906. https://doi.org/10.1002/pola.29074.

(64) Hua, G.; Franzén, J.; Odelius, K. Phosphazene-Catalyzed Regioselective Ring-Opening Polymerization of Rac-1-Methyl Trimethylene Carbonate: Colder and Less Is Better. *Macromolecules* **2019**, *52*, 2681–2690. https://doi.org/10.1021/acs.macromol.8b02591.

(65) Gregory, G. L.; Ulmann, M.; Buchard, A. Synthesis of 6-Membered Cyclic Carbonates from

1,3-Diols and Low CO2 Pressure: A Novel Mild Strategy to Replace Phosgene Reagents. *RSC Adv*. **2015**, *5*, 39404–39408. https://doi.org/10.1039/C5RA07290E.

(66) Ortmann, P.; Mecking, S. Long-Spaced Aliphatic Polyesters. *Macromolecules* **2013**, *46*, 7213–7218. https://doi.org/10.1021/ma401305u.

(67) Miller, S. A.; Thi, H.; Nguyen, H.; Qi, P.; Rostagno, M.; Feteha, A. Materials Chemistry A Materials for Energy and Sustainability The Quest for High Glass Transition Temperature Bioplastics. **2018**, *6*, 9283–9748. https://doi.org/10.1039/c8ta00377g.

(68) Sousa, A. F.; Vilela, C.; Fonseca, A. C.; Matos, M.; Freire, C. S. R.; Gruter, G. J. M.; Coelho, J. F. J.; Silvestre, A. J. D. Biobased Polyesters and Other Polymers from 2,5-Furandicarboxylic Acid: A Tribute to Furan Excellency. *Polym. Chem.* **2015**, *6*, 5961–5983. https://doi.org/10.1039/c5py00686d.

(69) Morales-Huerta, J. C.; Martínez De Ilarduya, A.; Muñoz-Guerra, S. Sustainable Aromatic Copolyesters via Ring Opening Polymerization: Poly(Butylene 2,5-Furandicarboxylate-Co-Terephthalate)S. *ACS Sustain. Chem. Eng.* **2016**, *4*, 4965–4973. https://doi.org/10.1021/acssuschemeng.6b01302.

(70) Li, J.; Stayshich, R. M.; Meyer, T. Y. Exploiting Sequence To Control the Hydrolysis Behavior of Biodegradable PLGA Copolymers. *J. Am. Chem. Soc.* **2011**, *133*, 6910–6913. https://doi.org/10.1021/ja200895s.

(71) Stayshich, R. M.; Weiss, R. M.; Li, J.; Meyer, T. Y. Periodic Incorporation of Pendant Hydroxyl Groups in Repeating Sequence PLGA Copolymers. *Macromol. Rapid Commun.* **2011**, *32*, 220–225. https://doi.org/10.1002/marc.201000608.

(72) Washington, M. A.; Swiner, D. J.; Bell, K. R.; Fedorchak, M. V.; Little, S. R.; Meyer, T. Y. The Impact of Monomer Sequence and Stereochemistry on the Swelling and Erosion of

Biodegradable Poly(Lactic-Co-Glycolic Acid) Matrices. *Biomaterials* **2017**, *117*, 66–76. https://doi.org/10.1016/j.biomaterials.2016.11.037.

(73) Weiss, R. M.; Short, A. L.; Meyer, T. Y. Sequence-Controlled Copolymers Prepared via Entropy-Driven Ring-Opening Metathesis Polymerization. *ACS Macro Lett*. **2015**, *4*, 1039–1043. https://doi.org/10.1021/acsmacrolett.5b00528.

(74) Brandrup, J.; Immergut, E.; Grulke, E. A. Polymer Handbook. *John Wiley Sons, Inc* **1990**, *12*, 265. https://doi.org/10.1016/0168-3659(90)90108-6.

(75) Chae, T. U.; Ahn, J. H.; Ko, Y. S.; Kim, J. W.; Lee, J. A.; Lee, E. H.; Lee, S. Y. Metabolic Engineering for the Production of Dicarboxylic Acids and Diamines. *Metab. Eng*. **2020**, *58*, 2–16. https://doi.org/10.1016/j.ymben.2019.03.005.

(76) Liang, G.; Wu, J.; Gao, H.; Wu, Q.; Lu, J.; Zhu, F.; Tang, B. Z. General Platform for Remarkably Thermoresponsive Fluorescent Polymers with Memory Function. *ACS Macro Lett*. **2016**, *5*, 909–914. https://doi.org/10.1021/acsmacrolett.6b00453.

(77) Nagarajan, S.; Sankar, V.; Bejoymohandas, K. S.; Duan, Y.; Zhang, J. Influence of Branched Polyester Chains on the Emission Behavior of Dipyridamole Molecule and Its Biosensing Ability. *ACS Omega* **2018**, *3*, 15530–15537. https://doi.org/10.1021/acsomega.8b01436.

(78) Reineke, T. M. Stimuli-Responsive Polymers for Biological Detection and Delivery. *ACS Macro Lett*. **2016**, *5*, 14–18. https://doi.org/10.1021/acsmacrolett.5b00862.

(79) Zeng, B.; Li, Y.; Wang, L.; Zheng, Y.; Shen, J.; Guo, S. Body Temperature-Triggered Shape-Memory Effect via Toughening Sustainable Poly(Propylene Carbonate) with Thermoplastic Polyurethane: Toward Potential Application of Biomedical Stents. *ACS Sustain. Chem. Eng*. **2020**, *8*, 1538–1547. https://doi.org/10.1021/acssuschemeng.9b06080.

(80) Ajili, S. H.; Ebrahimi, N. G.; Soleimani, M. Polyurethane/Polycaprolactane Blend with Shape Memory Effect as a Proposed Material for Cardiovascular Implants. *Acta Biomater*. **2009**, *5*, 1519–1530. https://doi.org/10.1016/j.actbio.2008.12.014.

(81) Xue, L.; Dai, S.; Li, Z. Synthesis and Characterization of Elastic Star Shape-Memory Polymers as Self-Expandable Drug-Eluting Stents. *J. Mater. Chem.* **2012**, *22*, 7403–7411. https://doi.org/10.1039/c2jm15918j.

(82) Mialon, L.; Vanderhenst, R.; Pemba, A. G.; Miller, S. A. Polyalkylenehydroxybenzoates (PAHBs): Biorenewable Aromatic/Aliphatic Polyesters from Lignin. *Macromol. Rapid Commun.* **2011**, *32*, 1386–1392. https://doi.org/10.1002/marc.201100242.

(83) Schutyser, W.; Renders, ab T.; Van den Bosch, S.; Koelewijn, S.; Beckham, G. T.; Sels, B. F. Chemicals from Lignin: An Interplay of Lignocellulose Fractionation, Depolymerisation, and Upgrading. *Chem. Soc. Rev* **2018**, *47*, 908. https://doi.org/10.1039/c7cs00566k.

(84) Llevot, A.; Grau, E.; Carlotti, S.; Grelier, S.; Cramail, H. From Lignin-Derived Aromatic Compounds to Novel Biobased Polymers. *Macromol. Rapid Commun.* **2016**, *37*, 9–28. https://doi.org/10.1002/marc.201500474.

(85) Armarego, W. L. F.; Chai, C. *Purification of Laboratory Chemicals*; 2009. https://doi.org/10.1016/C2009-0-26589-5.

(86) Ito, M.; Nakamura, F.; Baba, A.; Kaoru, T.; Ushijima, H.; Lau, K. H. A.; Manna, A.; Knoll, W. Enhancement of Surface Plasmon Resonance Signals by Gold Nanoparticles on High-Density DNA Microarrays. *J. Phys. Chem. C* **2007**, *111*, 11653–11662. https://doi.org/10.1021/jp070524m.

(87) Steinmetz, H.; Li, J.; Fu, C.; Zaburannyi, N.; Kunze, B.; Harmrolfs, K.; Schmitt, V.; Herrmann, J.; Reichenbach, H.; Höfle, G.; Kalesse, M.; Müller, R. Isolation, Structure

Elucidation, and (Bio)Synthesis of Haprolid, a Cell-Type-Specific Myxobacterial Cytotoxin. *Angew. Chem. - Int. Ed.* **2016**, *55*, 10113–10117. https://doi.org/10.1002/anie.201603288.

(88) Bender, J. L.; Shen, Q.-D.; Fraser, C. L. Poly(ε-Caprolactone) Macroligands with β-Diketonate Binding Sites: Synthesis and Coordination Chemistry. *Tetrahedron* **2004**, *60*, 7277–7285. https://doi.org/10.1016/j.tet.2004.06.019.